DOT/FAA/CT-94/90
DOT-VNTSC-FAA-94-4

FAA Technical Center
Atlantic City International Airport,
N.J. 08405

Estimate of Probability of Crack Detection from Service Difficulty Report Data

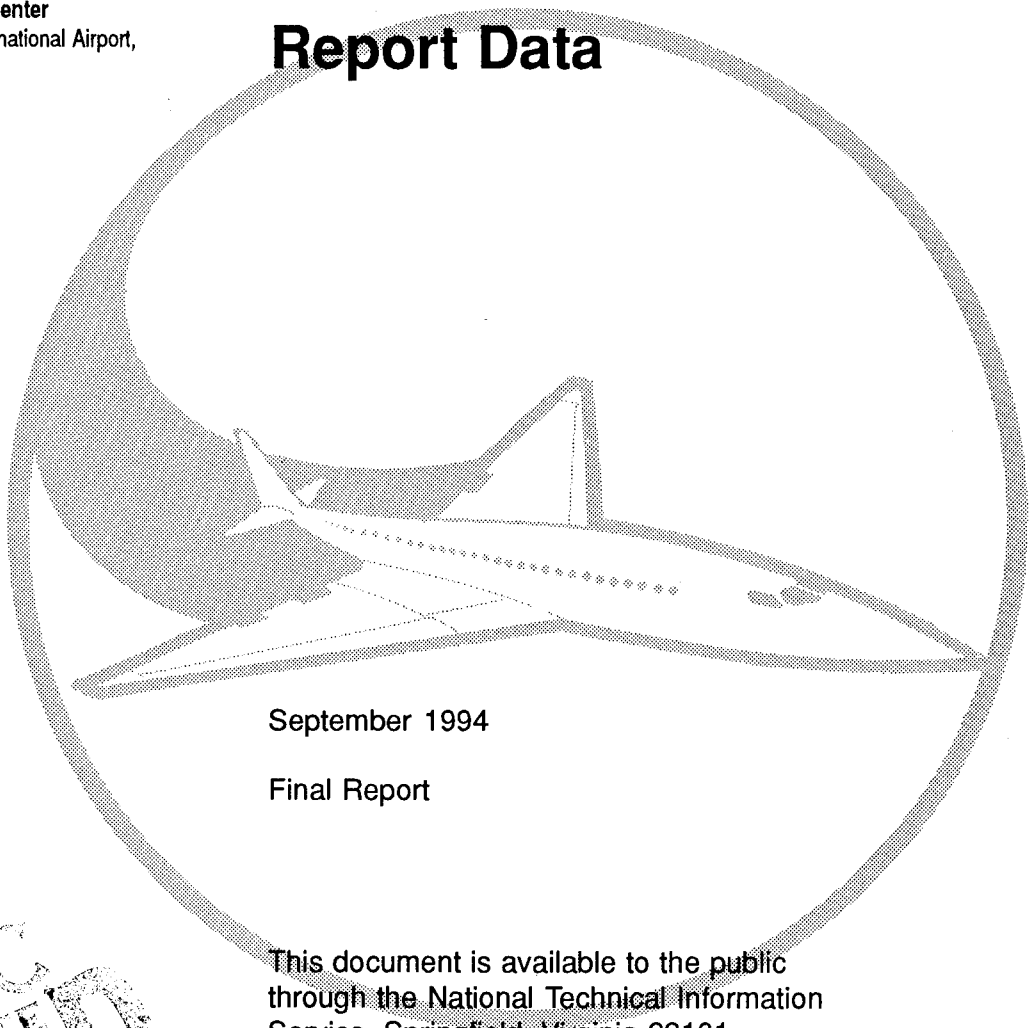

September 1994

Final Report

This document is available to the public through the National Technical Information Service, Springfield, Virginia 22161.

DTIC
ELECTE
DEC 07 1994
S F D

DISTRIBUTION STATEMENT A
Approved for public release;
Distribution Unlimited

U.S. Department of Transportation
Federal Aviation Administration

19941129 080

NOTICE

This document is disseminated under the sponsorship of the Department of Transportation in the interest of information exchange. The United States Government assumes no liability for its contents or use thereof.

REPORT DOCUMENTATION PAGE

Form Approved
OMB No. 0704-0188

Public reporting burden for this collection of information is estimated to average 1 hour per response, including the time for reviewing instructions, searching existing data sources, gathering and maintaining the data needed, and completing and reviewing the collection of information. Send comments regarding this burden estimate or any other aspect of this collection of information, including suggestions for reducing this burden, to Washington Headquarters Services, Directorate for information Operations and Reports, 1215 Jefferson Davis Highway, Suite 1204, Arlington, VA 22202-4302, and to the Office of Management and Budget, Paperwork Reduction Project (0704-0188), Washington, DC 20503.

1. AGENCY USE ONLY (Leave blank)

2. REPORT DATE
September 1994

3. REPORT TYPE AND DATES COVERED
Final Report
October 1992 - October 1993

4. TITLE AND SUBTITLE
Estimate of Probability of Crack Detection from Service Difficulty Report Data

5. FUNDING NUMBERS
FA4H2/A4044

6. AUTHOR(S)
John C. Brewer

7. PERFORMING ORGANIZATION NAME(S) AND ADDRESS(ES)
U.S. Department of Transportation
Research and Special Programs Administration
John A. Volpe National Transportation Systems Center
Cambridge, MA 02142

8. PERFORMING ORGANIZATION REPORT NUMBER
DOT-VNTSC-FAA-94-4

9. SPONSORING/MONITORING AGENCY NAME(S) AND ADDRESS(ES)
U.S. Department of Transportation
Federal Aviation Administration Technical Center
Atlantic City International Airport, NJ 08405

10. SPONSORING/MONITORING AGENCY REPORT NUMBER
DOT/FAA/CT-94/90

11. SUPPLEMENTARY NOTES

12a. DISTRIBUTION/AVAILABILITY STATEMENT
This document is available to the public through the National Technical Information Service, Springfield, VA 22161

12b. DISTRIBUTION CODE

13. ABSTRACT (Maximum 200 words)

The initiation and growth of cracks in a fuselage lap joint were simulated. Stochastic distributions of crack initiation and rivet interference were included. The simulation also contained a simplified crack link-up criterion and the effect of rivet interference on crack growth. Nominal crack growth behavior of large cracks was derived from the simulation results. These calculations implied that large cracks spend most of their lives as multiple small cracks and that the final growth and coalescence occur rapidly. The nominal crack growth histories were applied to "C-check" crack detection data from the Service Difficulty Report (SDR) database to estimate the sizes of cracks when they were missed during previous inspections. These "nondetection events" were also estimated by assuming that each detected crack had always been a single crack. The results of each method were appropriately filtered and used to estimate probability of crack detection (POD) using the maximum likelihood technique. The POD estimates obtained from the single crack model are probably conservative, but the underlying assumption of slow crack growth (and therefore more inspection opportunities) might result in unconservative damage tolerance analyses.

14. SUBJECT TERMS
Probability of Detection, Non-Destructive Inspection, Crack Growth, Visual Inspection, Damage Tolerance, Service Difficulty Reports, Widespread Fatigue Damage, "C-Check", Fuselage Lap Joint, Aircraft Maintenance

15. NUMBER OF PAGES
52

16. PRICE CODE

17. SECURITY CLASSIFICATION OF REPORT
Unclassified

18. SECURITY CLASSIFICATION OF THIS PAGE
Unclassified

19. SECURITY CLASSIFICATION OF ABSTRACT
Unclassified

20. LIMITATION OF ABSTRACT

PREFACE

The present work was performed at the John A. Volpe National Transportation Systems Center (Volpe Center) in Cambridge, MA. The task is part of a Project Plan Agreement (PPA) between the Federal Aviation Administration Technical Center (FAATC) in Atlantic City, NJ and the Volpe Center. The PPA is entitled "Structural Integrity of Aging Airframes."

The task that addresses probability of crack detection and aircraft systems reliability seeks to combine results of several facets of the FAATC Aging Aircraft Program. The purpose is to assess the suitability of various methods for determining and using probability of crack detection functions in damage tolerance analyses of transport aircraft.

The author wishes to thank Dr. Chris Smith, Mr. Chris Seher, Mr. Eugene Klueg, Dr. Sam Sampath, and Dr. D. Scott Pipkins of FAATC for their contributions to and support of this effort.

Accession For
NTIS GRA&I ☑
DTIC TAB ☐
Unannounced ☐
Justification
By
Distribution/
Availability Codes
Dist | Avail and/or Special
A-1

METRIC/ENGLISH CONVERSION FACTORS

ENGLISH TO METRIC

LENGTH (APPROXIMATE)

1 inch (in) = 2.5 centimeters (cm)
1 foot (ft) = 30 centimeters (cm)
1 yard (yd) = 0.9 meter (m)
1 mile (mi) = 1.6 kilometers (km)

AREA (APPROXIMATE)

1 square inch (sq in, in^2 = 6.5 square centimeters (cm^2)
1 square foot (sq ft, ft^2 = 0.09 square meter (m_2)
1 square yard (sq yd, yd^2) = 0.8 square meter (m^2)
1 square mile (sq mi, mi^2) = 2.6 square kilometers (km^2)
1 acre = 0.4 hectares (he) = 4,000 square meters (m^2)

MASS - WEIGHT (APPROXIMATE)

1 ounce (oz) = 28 grams (gr)
1 pound (lb) = .45 kilogram (kg)
1 short ton = 2,000 pounds (lb) = 0.9 tonne (t)

VOLUME (APPROXIMATE)

1 teaspoon (tsp) = 5 milliliters (ml)
1 tablespoon (tbsp) = 15 milliliters (ml)
1 fluid ounce (fl oz) = 30 milliliters (ml)
1 cup (c) = 0.24 liter (1)
1 pint (pt) = 0.47 liter (1)
1 quart (qt) = 0.96 liter (1)
1 gallon (gal) = 3.8 liters (1)
1 cubic foot (cu ft, ft^3) = 0.03 cubic meter (m^3)
1 cubic yard (cu yd, yd^3) = 0.76 cubic meter (m^3)

TEMPERATURE (EXACT)

$[(x-32)(5/9)]\ ^{o}F = y\ ^{o}C$

METRIC TO ENGLISH

LENGTH (APPROXIMATE)

1 millimeter (mm) = 0.04 inch (in)
1 centimeter (cm) = 0.4 inch (in)
1 meter (m) = 3.3 feet (ft)
1 meter (m) = 1.1 yards (yd)
1 kilometer (km) = 0.6 mile (mi)

AREA (APPROXIMATE)

1 square centimeter (cm^2) = 0.16 square inch (sq in, in^2)
1 square meter (m^2) = 1.2 square yeards (sq yd, yd^2)
1 square kilometer (km^2) = 0.4 square mile (sq mi, mi^2)
1 hectare (he) = 10,000 square meters (m^2) = 2.5 acres

MASS - WEIGHT (APPROXIMATE)

1 gram (gr) = 0.036 ounce (oz)
1 kilogram (kg) = 2.2 pounds (lb)
1 tonne (t) = 1,000 kilograms (kg) = 1.1 short tons

VOLUME (APPROXIMATE)

1 milliliters (ml) = 0.03 fluid ounce (fl oz)
1 liter (1) = 2.1 pints (pt)
1 liter (1) = 1.06 quarts (qt)
1 liter (1) = 0.26 gallon (gal)
1 cubic meter (m^3) = 36 cubic feet (cu ft, ft^3)
1 cubic meter (m^3) = 1.3 cubic yards (cu yd, yd^3)

TEMPERATURE (EXACT)

$[(9/5)\ y + 32]\ ^{o}C = x\ ^{o}F$

QUICK INCH-CENTIMETER LENGTH CONVERSION

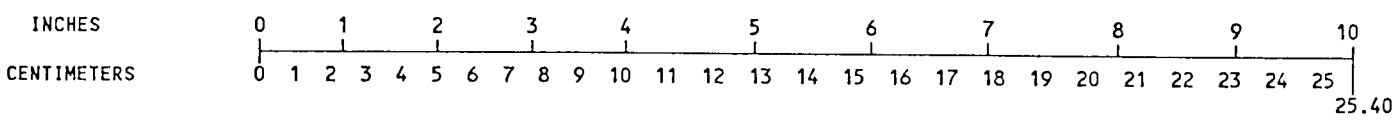

QUICK FAHRENHEIT-CELSIUS TEMPERATURE CONVERSION

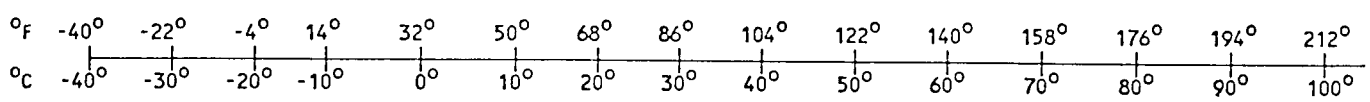

For more exact and or other conversion factors, see NBS Miscellaneous Publication 286, Units of Weights and Measures. Price $2.50. SD Catalog No. C13 10286.

TABLE OF CONTENTS

Section		Page
1.	INTRODUCTION	1
2.	CRACK GROWTH SIMULATION	7
	2.1 Components of the Simulation	7
	2.2 Results of the Simulation	13
	2.3 Discussion of the Simulation	13
3.	NOMINAL CRACK GROWTH HISTORIES	17
	3.1 Determination of Nominal Crack Growth Histories	17
	3.2 Discussion of Nominal Crack Growth Histories	17
4.	ANALYSIS OF DATA FROM SERVICE DIFFICULTY REPORTS	19
	4.1 The Service Difficulty Report Database	19
	4.2 Application of the "Keep Region"	20
	4.3 Maximum Likelihood Estimate of Probability of Detection	21
	4.4 Discussion of the Maximum Likelihood Estimates	23
5.	CONCLUSIONS AND RECOMMENDATIONS	29
REFERENCES		31
APPENDIX A -	NOMINAL CRACK SIZES (DOWN TO 0.1") THAT PRECEDE OBSERVED CRACKS	33

LIST OF ILLUSTRATIONS

Figure		Page
1-1	SCHEMATIC OF DETECTION AND NONDETECTION EVENTS . .	2
1-2	ILLUSTRATION OF THE "KEEP REGION" OF VALID DETECTION AND NONDETECTION EVENTS	3
1-3	DEFINITION OF "LIKELIHOOD" OF AN EVENT	4
1-4	COMPARISON OF SIMPLE (UPPER) AND SOPHISTICATED CRACK GROWTH MODELS	5
2-1	FLOW CHART FOR THE SIMULATION OF CRACK FORMATION AND GROWTH	8
2-2	SCHEMATIC OF A TEN-INCH BAY OF A FUSELAGE LAP JOINT	9
2-3	SCHEMATIC OF TWO CRACKS BEFORE LINKUP	12
2-4	DEFINITION OF MAXIMUM PRECURSOR LENGTH	13
2-5	DEFINITION OF CRACK REINITIATION	14
2-6	CRACK SIZE DISTRIBUTION IN A FATIGUE TEST OF A FULL-SCALE FUSELAGE PANEL	16
3-1	NOMINAL CRACK GROWTH HISTORY OF A FOUR-LIGAMENT CRACK	18
4-1	MAXIMUM LIKELIHOOD ESTIMATES OF POD FUNCTIONS USING THE NOMINAL CRACK GROWTH HISTORY METHODOLOGY	24
4-2	MAXIMUM LIKELIHOOD ESTIMATES OF POD FUNCTIONS USING THE WALKER CRACK GROWTH METHODOLOGY	25
4-3	COMPARISON OF THE PROBABILITY OF DETECTION CURVES FROM THE TWO METHODOLOGIES (LOGISTIC FIT ONLY) . .	26

LIST OF TABLES

Table		Page
2-1	RIVET LOADS IN THE LAP JOINT	10
2-2	WEIBULL PARAMETERS FOR INITIATION DAMAGE	10
2-3	AVERAGE RESULTS FOR THE ENTIRE BAY	14
2-4	AVERAGE RESULTS FOR LINKUPS	15
4-1	MINIMUM CRACK SIZES NECESSARY TO BE IN THE "KEEP REGION"	21
4-2	MAXIMUM LIKELIHOOD SHAPE AND LOCATION PARAMETERS FOR PROBABILITY OF DETECTION FUNCTIONS	23
4-3	HISTOGRAM ESTIMATES OF POD FOR NOMINAL CRACK GROWTH HISTORY METHODOLOGY	23
4-4	HISTOGRAM ESTIMATES OF POD FOR WALKER CRACK GROWTH METHODOLOGY	26
A-1	NOMINAL HISTORY OF A ONE-INCH CRACK	33
A-2	NOMINAL HISTORY OF A TWO-INCH CRACK	34
A-3	NOMINAL HISTORY OF A THREE-INCH CRACK	35
A-4	NOMINAL HISTORY OF A FOUR-INCH CRACK	36
A-5	NOMINAL HISTORY OF A FIVE-INCH CRACK	37
A-6	NOMINAL HISTORY OF A SIX-INCH CRACK	38
A-7	NOMINAL HISTORY OF A SEVEN-INCH CRACK	39
A-8	NOMINAL HISTORY OF AN EIGHT-INCH CRACK	40
A-9	NOMINAL HISTORY OF A NINE-INCH CRACK	41

EXECUTIVE SUMMARY

This report summarizes three analyses completed at the Volpe Center. The first was the development of a detailed simulation of crack initiation, growth, and linkup in typical fuselage lap joints. The second involved using the simulation to determine a typical or "nominal" history for detected cracks. The third used the nominal crack growth histories to estimate the in-service probability of crack detection from aircraft maintenance data.

The simulation examined a completely debonded ten-inch bay of a fuselage lap joint. The value of "damage" needed to initiate cracks was modeled as a random function. The degree of rivet interference was a function of the initiation damage. Crack growth was calculated with a form of the Walker equation. Linkup of multiple cracks was determined from the geometric parameters of the two linking cracks.

The simulations indicated that widespread fatigue damage could develop slowly and lead to rapid linkup. This may have significant ramifications for damage tolerance analyses because it implies that the probability of crack detection is extremely low during most inspections. The nominal crack growth histories were determined from the results of 10,000 simulations of crack growth in the bay. Parameters recorded during the simulations were used to characterize the nominal behavior of commonly occurring crack sizes.

The nominal crack growth histories were then applied to crack detection data retrieved from the Service Difficulty Report (SDR) database. By knowing the most likely history of a detected crack, its size at previous inspections can be inferred. The detection and nondetection events and their associated crack sizes were carefully censored to minimize the effect of relevant but unattainable data points (such as the nondetection events for cracks that had not yet been found at the closing of the database). The data were then used in a maximum likelihood estimate of the probability of crack detection functions.

The probability of detection results were compared to those of an analysis that used a simpler crack growth model. The simple model predicted slower, more steady growth. This implied more nondetection events at larger crack sizes and a generally lower probability of detection. Nonetheless, if a damage tolerance analysis relies on this slower crack growth, the lower probability of detection may not guarantee a conservative analysis.

The two probability of detection estimates may serve as practical bounds to the actual in-service values. It may be informative to estimate the in-service values with other methods to

ascertain whether the model that includes widespread fatigue damage is an improvement over the simple single-crack model.

1. INTRODUCTION

FAA Advisory Circular 25.571-1A states that damage tolerance means that the "structure has been evaluated to ensure that, should serious fatigue, corrosion, or accidental damage occur within the operational life of the airplane, the remaining structure can withstand reasonable loads without failure or excessive structural deformation until the damage is detected [1]." Thus, the probability of crack detection during inspection is an important component of damage tolerance evaluations of transport aircraft structures subject to fatigue. Laboratory evaluations of inspection techniques cannot always accurately represent the full range of influences on field inspections. Lighting, time of day, location and orientation of the crack, and the possibility that a location might not be inspected can serve to alter the effective probability of detection (POD).

One approach to ascertain the in-service POD is to infer it from maintenance data. The data needed to develop a POD curve are the crack sizes at the crack detection events and nondetection events of all inspections. The concept is illustrated in Figure 1-1. The complete inspection history for a specific aircraft (including all inspections when no cracks were found) is rarely accessible in the same database as the detected crack sizes. Thus, assumptions are generally made regarding the frequency and type of inspections. Since details of nondetection events are, by definition, not recorded, the events and the associated crack sizes must be deduced from a crack growth model. A more sophisticated and appropriate model would produce a more accurate POD curve.

There is a need to carefully censor detection and nondetection data [2]. The rationale is that detected cracks may have "siblings" which can contribute valid nondetection events to the dataset, as shown in Figure 1-2. A dataset that does not contain all pertinent detection and nondetection data would inappropriately skew the POD curve. This difficulty can be resolved by eliminating any crack detection event (and its associated nondetection events) from the data set if an identical crack could not be assured to have been found. Similarly, it would be improper to include nondetection events that occurred before the database opened since detection events associated with sibling cracks could not be counted. This defines the "keep region" shown in the figure.

The determination of a POD curve from the detection and nondetection data requires the selection of a functional form for the curve (e.g., log normal). The detection and nondetection events can then be used to compute the "likelihood" of the data. Likelihood of the dataset is the product of the individual probabilities of each event. That is, it is the product of probabilities of detection for each detection event times the

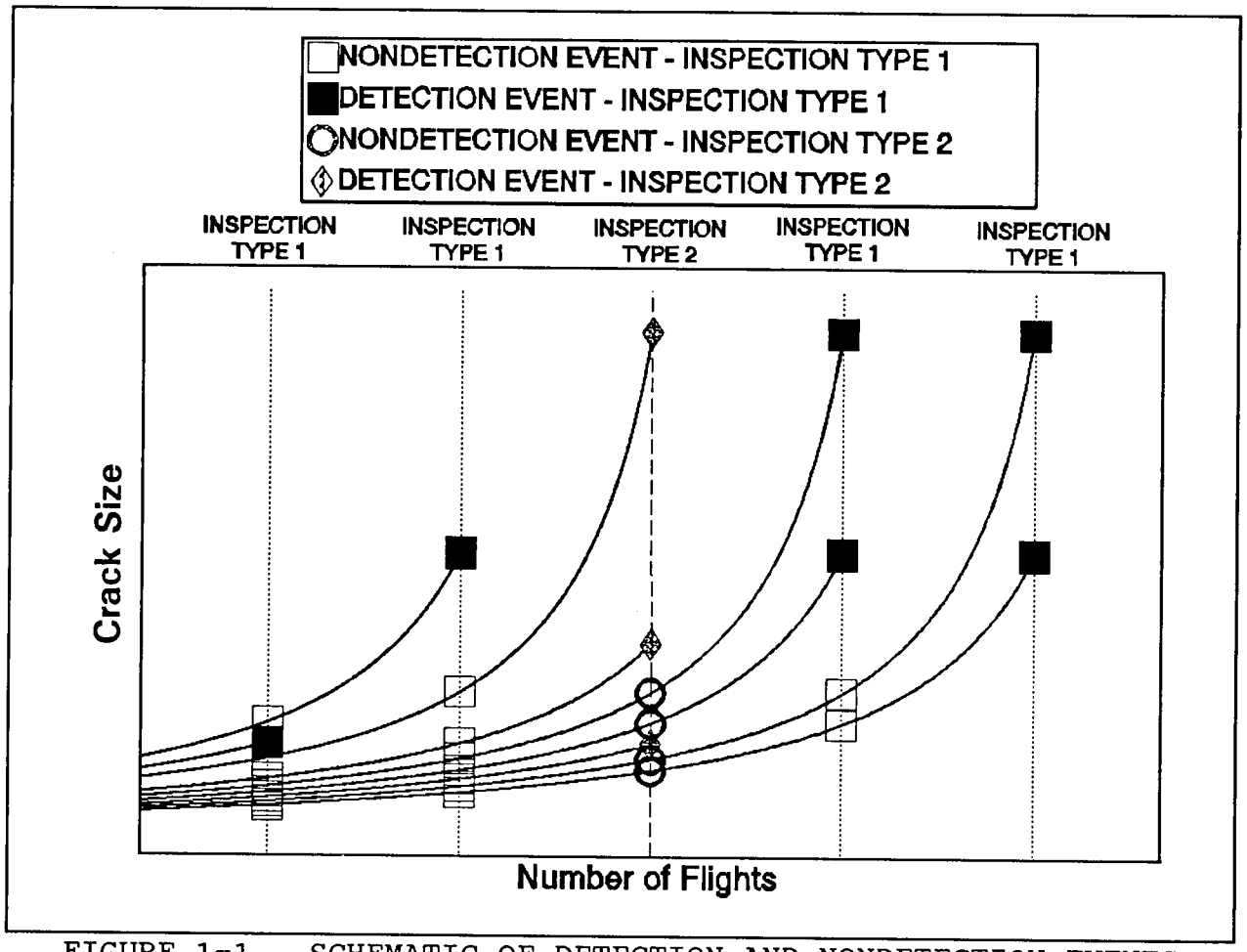

FIGURE 1-1. SCHEMATIC OF DETECTION AND NONDETECTION EVENTS

product of probabilities of nondetection for each nondetection event. The likelihood of an individual event is shown in Figure 1-3. The values of the parameters in the function can then be refined to achieve the maximum likelihood.

An appropriate POD methodology requires a realistic crack growth scenario. For example, if a Paris law approach were used, the crack growth parameter should be based on experimental data. Simple single crack models, however, do not adequately account for the fact that long cracks seldom grow steadily. The actual behavior includes several complex and, in some cases, stochastic mechanisms. These include crack initiation, rivet interference, and crack linkup. Thus, a long crack may well have been several short cracks instead of one medium-size crack at a previous inspection. Figure 1-4 compares a simple crack growth model with a more sophisticated one.

This report describes a simulation of the complex interactions that influence crack size as a function of time and draws conclusions about the "nominal" behavior of a detected crack. That

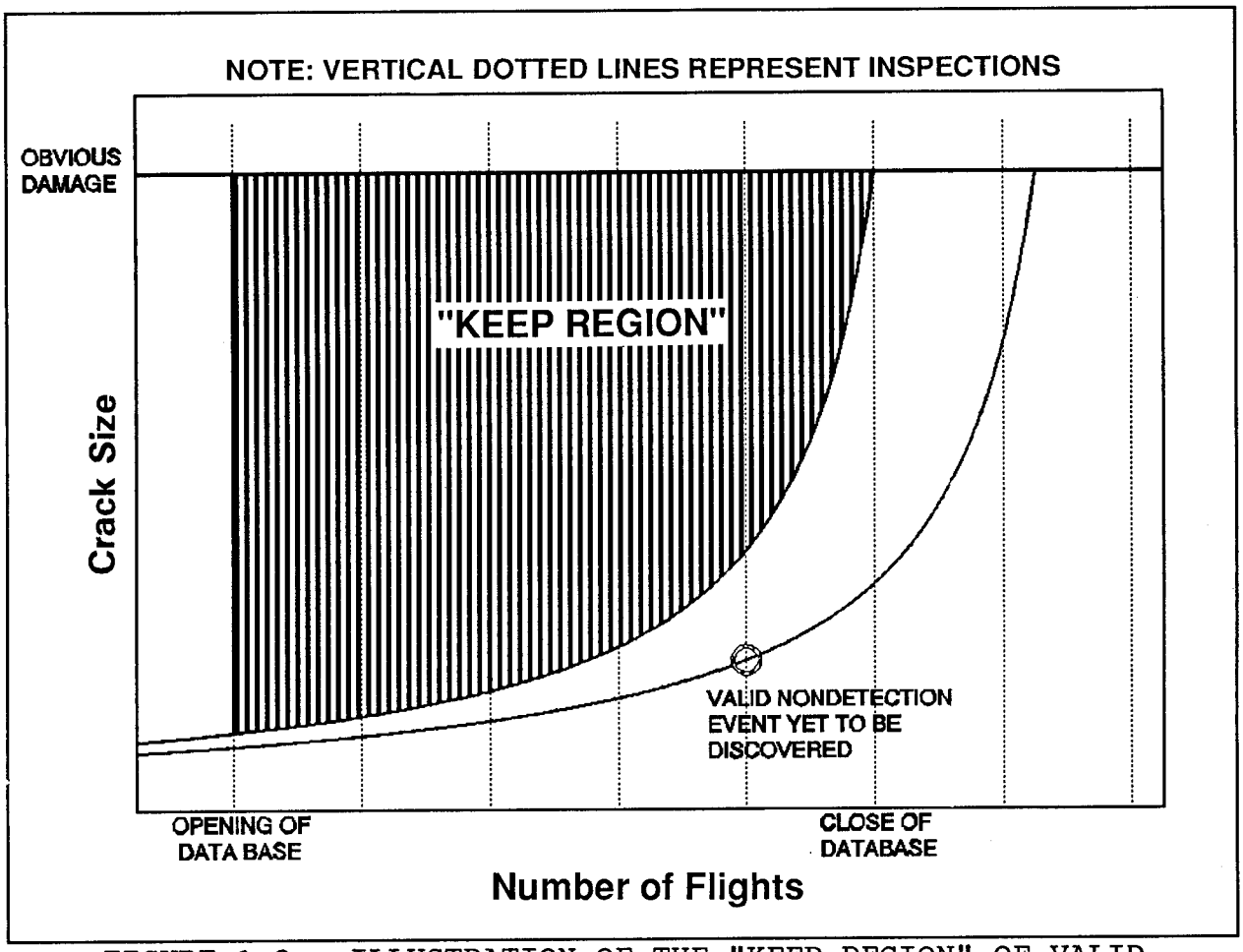

FIGURE 1-2. ILLUSTRATION OF THE "KEEP REGION" OF VALID DETECTION AND NONDETECTION EVENTS

is, the proposed methodology produces a typical or most likely crack growth scenario for certain commonly detected crack sizes. The simulation of crack growth includes crack initiation, rivet interference, and linkup models. The reduction of the simulation results to nominal crack histories will be discussed. The methodology is then applied to a group of cracks extracted from the FAA's Service Difficulty Reporting database. POD curves are derived using the proposed methodology and a simple, more conventional crack growth equation.

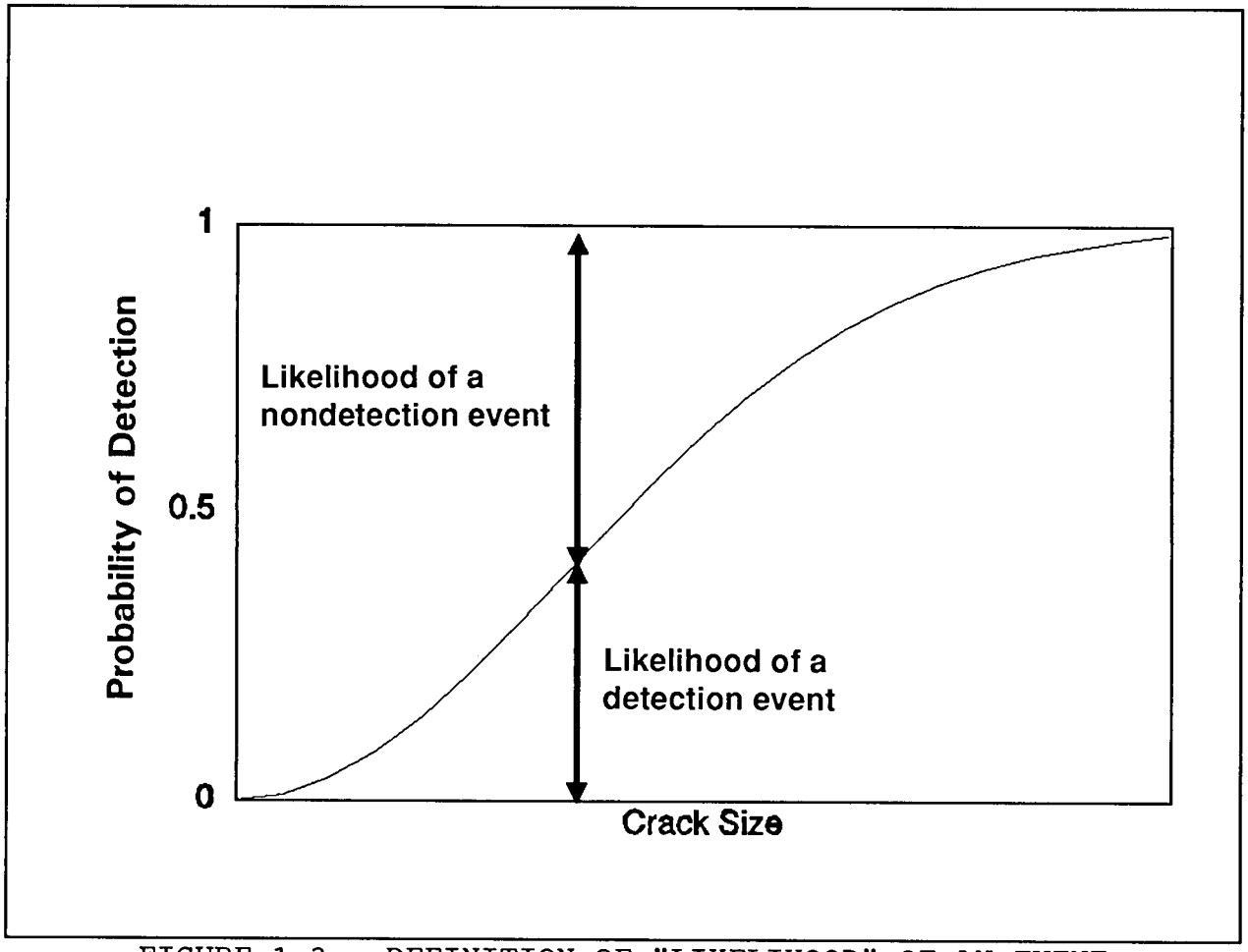

FIGURE 1-3. DEFINITION OF "LIKELIHOOD" OF AN EVENT

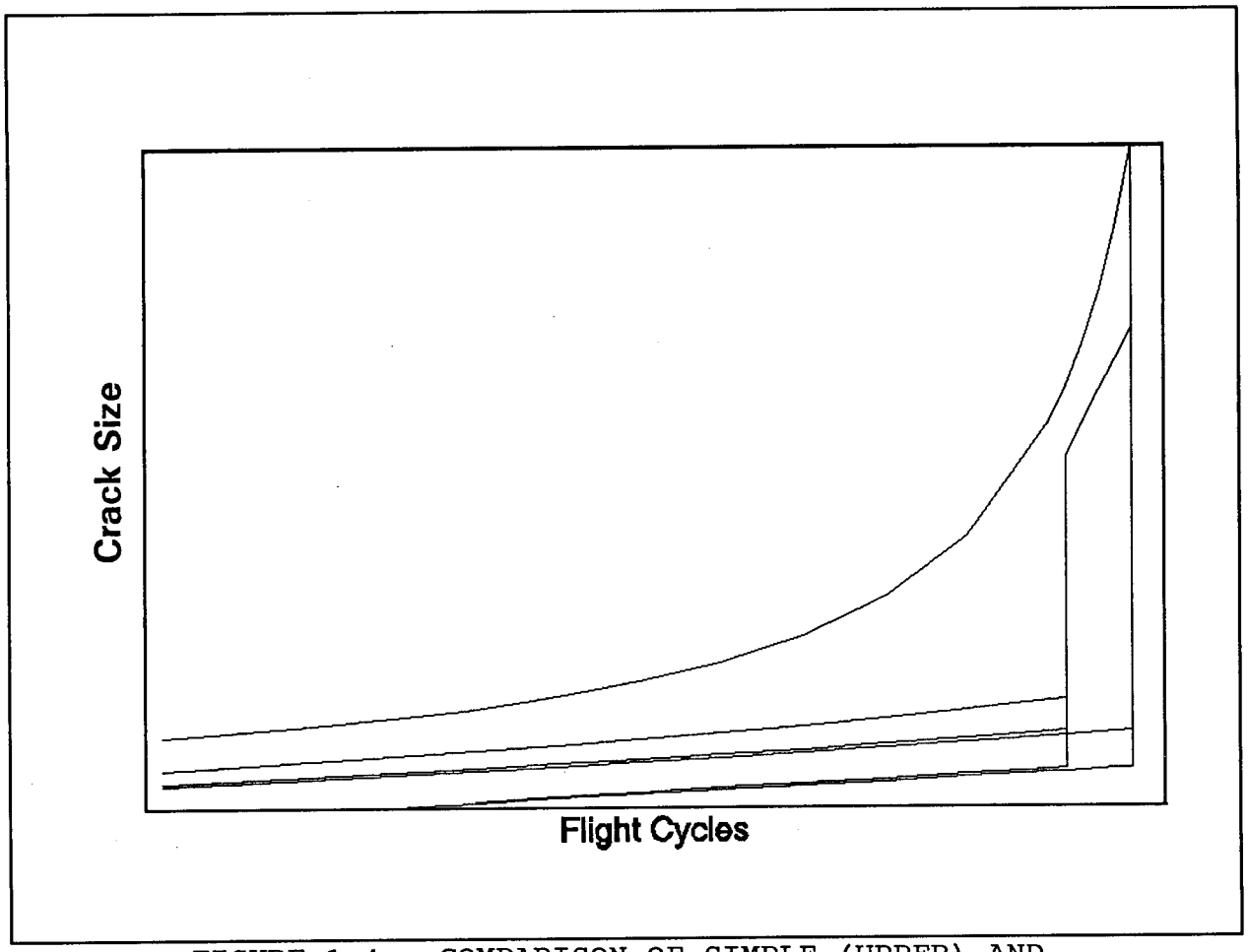

FIGURE 1-4. COMPARISON OF SIMPLE (UPPER) AND SOPHISTICATED CRACK GROWTH MODELS

2. CRACK GROWTH SIMULATION

2.1 COMPONENTS OF THE SIMULATION

The nominal crack growth methodology requires numerous simulations of crack growth in a typical bay. Each simulation trial must consider the various deterministic and stochastic effects mentioned above. A flow chart of the simulation is shown in Figure 2-1.

The first element of the crack growth simulation was the stress distribution across the representative ten-inch wide bay illustrated in Figure 2-2. The stress distribution was derived from a finite element model of the generic structure of a Boeing 737 fuselage section [3]. The load transfer across a lap joint was assumed to be entirely carried by the rivets rather than adhesive. This presumes complete debonding of the lap joint across the entire bay. More advanced versions of the simulation could account for progressive bond failure, if available data sufficiently describes this behavior in the fleet.

Load was taken to be uniform across a ligament. The loads transferred by a rivet were drawn from the ligaments on either side. It was assumed that half the rivet load was drawn from the ligament on the left and the other half was drawn from the ligament on the right. The rivet loads are given in Table 2-1 for a pressurization of 7.5 psi. It is the upper row of rivets that is most critical for cracking. In those cases in which one or more ligaments cracked and linked up, the load from the cracked ligament was assumed to have been transferred to the nearest ligament. If it were halfway between two unlinked ligaments, the load would be split between them.

The simulation required a method for simulating crack initiation. This process was modeled using the approach of Broek [4]. He proposed that a crack "initiated" (i.e., emerged from under the rivet head) when Miner's damage, D, reached a critical value for that crack location. Here, D is defined:

$$D = \Sigma\left(\frac{n_i}{N_i}\right) \tag{2-1}$$

where n_i is the number of cycles experienced at stress level i and N_i is the average fatigue life of a lap joint specimen at that

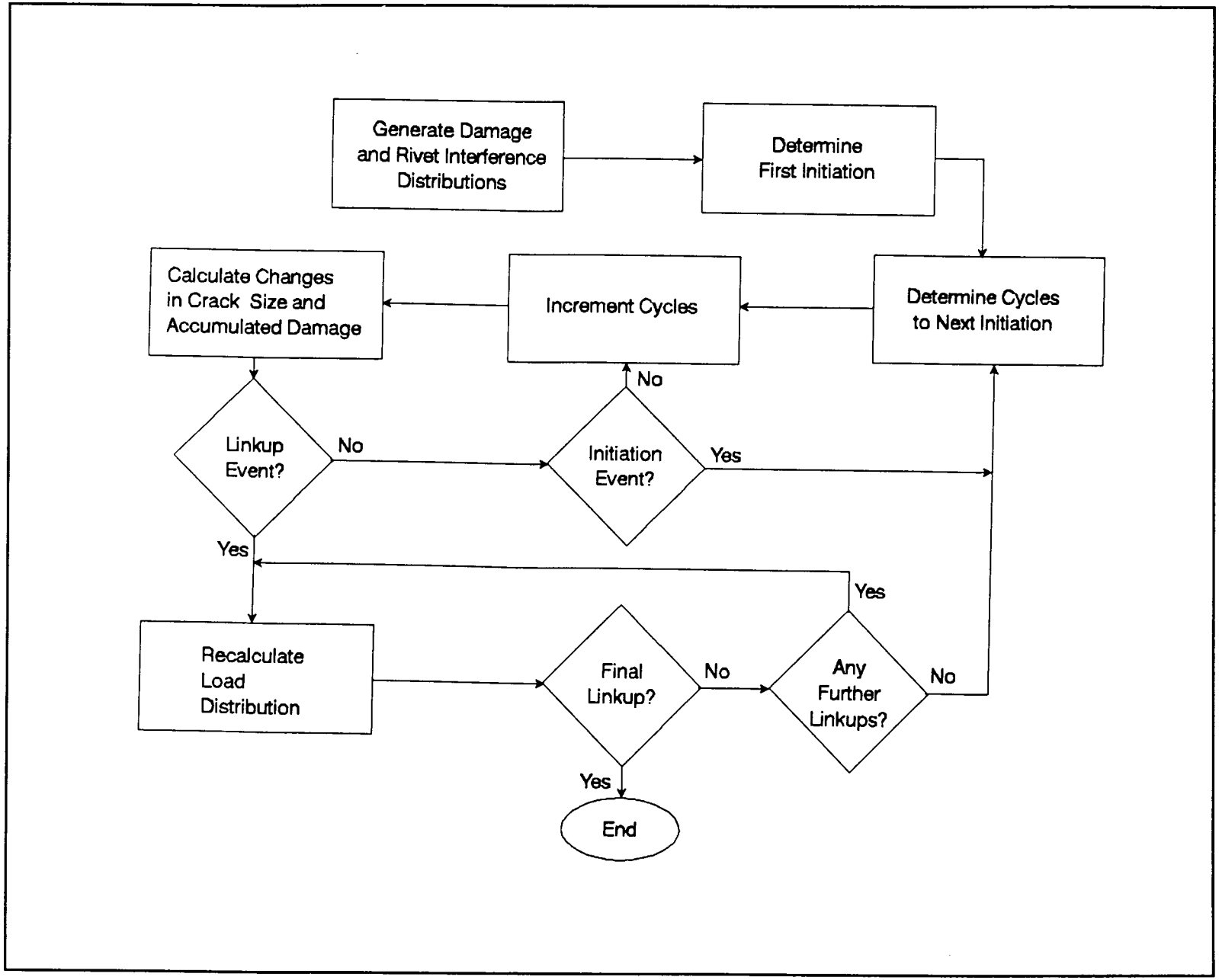

FIGURE 2-1. FLOW CHART FOR THE SIMULATION OF CRACK FORMATION AND GROWTH

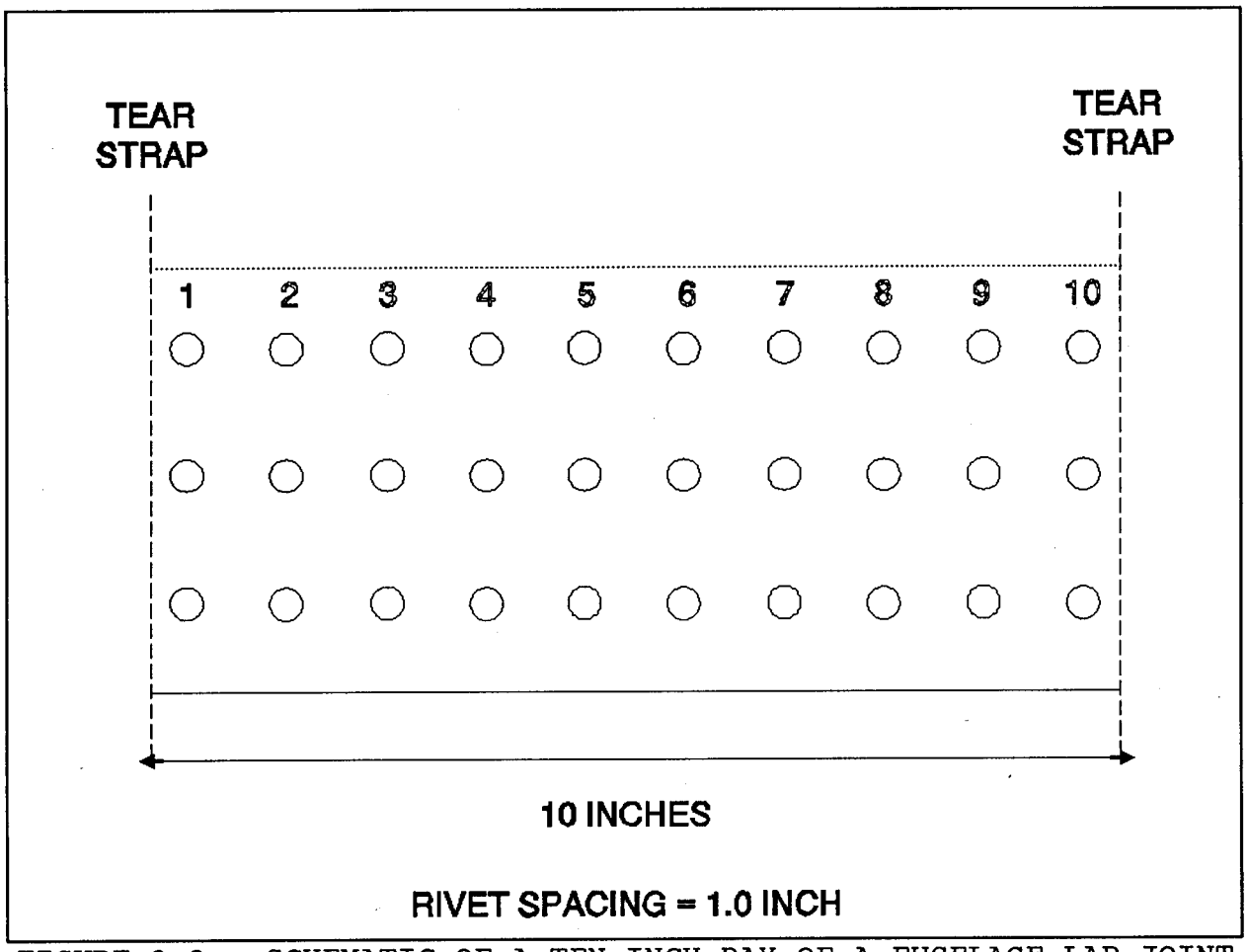

FIGURE 2-2. SCHEMATIC OF A TEN-INCH BAY OF A FUSELAGE LAP JOINT

stress level. N_i was given by the following equation:

$$N_i = \exp\left(\frac{43\ ksi - (\Delta\sigma)_i}{2.74\ ksi}\right) \tag{2-2}$$

In his analysis, Broek showed reasonable agreement with two sets of data [5,6] by assuming that the critical value of D would be randomly distributed. He fit the data with a three-parameter Weibull distribution. The values of the parameters he used are given in Table 2-2. These were the same values used in the present analysis. A random number generator was used to select a critical value of D for each crack location.

The crack growth model in Reference 7 was used for the crack growth in the simulation. Crack growth can be influenced significantly by the degree to which the rivet interferes with its hole [2,7]. A larger degree of interference will result in higher residual stresses around the circumference and, most likely,

TABLE 2-1. RIVET LOADS IN THE LAP JOINT

Hole Location	Upper Row Load [lbs]	Middle Row Load [lbs]	Bottom Row Load [lbs]	Total Load [lbs]
1,10	156	73	109	338
2,9	172	88	159	418
3,8	172	92	167	431
4,7	173	94	171	439
5,6	174	96	174	443

Note: Positions 1 and 10 are closest to the tear straps and frames. Positions 5 and 6 are centered between neighboring tear straps. Totals may not agree as a result of rounding.

TABLE 2-2. WEIBULL PARAMETERS FOR INITIATION DAMAGE

Minimum Value	0.5
Scale Parameter, λ_D	1.0
Shape Parameter, α_D	2.0

earlier crack initiation. The data presented in Reference 7 was reanalyzed to ascertain the number of cycles at which the crack would have just emerged from a 4.94 mm rivet head (the size used in the initiation data from Reference 5). The central four rivets from each specimen in Reference 7 were used because there was less uncertainty and scatter. The rivet interference (as calculated in Reference 7) was correlated with the damage, D, at "initiation" and yielded the following distribution of rivet interference, δ_o, with respect to damage:

$$\delta_o = -2.507 \times 10^{-4} in \cdot D + 2.287 \times 10^{-4} in \qquad (2\text{-}3)$$

In this simulation, the values of the damage, D, on either side of a rivet were averaged and the equation above was applied to assign a value of δ_o to the rivet. Negative values of δ_o are physically equivalent to values of 0.0 because they imply no interference at all.

The crack growth equation was the following version of the Walker equation as recommended in Reference 8:

$$\frac{da}{dN} = \frac{2.5 \times 10^{-10}\, ksi^{-4}\, in^{-1}\, (\Delta K)^4}{1 - R} \tag{2-4}$$

where a is the crack length parameter, N is the number of cycles, K is the stress intensity factor, and R is the stress ratio of the cycle. An effective value of R was used because rivet interference sometimes altered the maximum and minimum stress intensity factors at the crack tips. Thus, R was equal to the ratio of minimum to maximum stress intensity factor instead of the ratio of minimum to maximum far field stress:

$$R_{eff} = \frac{K_I^{min}}{K_I^{max}} \tag{2-5}$$

The final aspect of the simulation involved crack linkup or, equivalently, ligament failure. Linkup was based on the stress in the net section of the ligament. Partl and Schijve [9] have suggested that significant interaction of cracks does not take place until the ligament length is less than half the distance between rivet centers. Because of the fast crack growth at this crack size, it might be argued that precise determination of the linkup event may not be necessary in general analyses. Nonetheless, in this simulation, it is necessary to ascertain the capacity of a ligament to withstand the extra load it would bear following the failure of a neighboring ligament.

Foster-Miller, Inc. has tested specimens with the potential for multiple linkups [10]. A simple net section criterion did not adequately correlate the preliminary data. For the purposes of the present simulation, a trend analysis was sufficient. It showed that the linkup data was well represented by the equation:

$$\sqrt{\frac{c}{l}}\, \sigma_o = 44.08\ ksi \approx \sigma_{yield} \tag{2-6}$$

where σ_o is the far field applied stress, c is the distance between the centers of the neighboring cracks, and l is the length of the ligament. This configuration is illustrated in Figure 2-3.

The simulation was implemented on a personal computer. At each stage of the simulation, the number of cycles to the next initiation event was calculated. Crack growth was allowed to proceed in blocks of up to 125 cycles. After the crack growth from the block was computed, each ligament was analyzed to see if linkup would occur. Whenever linkup occurred, the load redistribution was calculated and the remaining ligaments were reanalyzed. The program recorded the number of cycles associated with each crack initiation

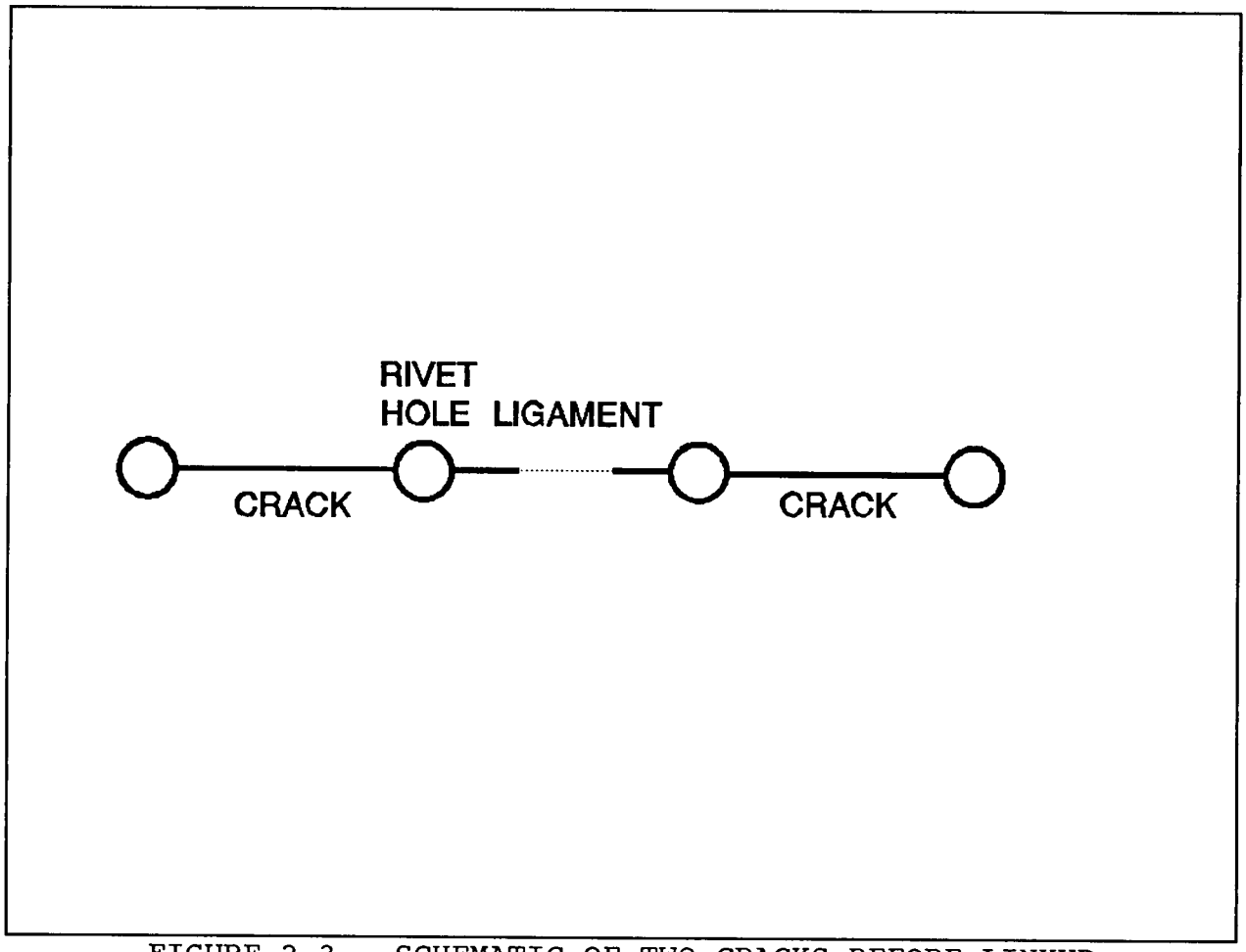

FIGURE 2-3. SCHEMATIC OF TWO CRACKS BEFORE LINKUP

and linkup event. It also recorded the maximum precursor length associated with each linkup event. The maximum precursor length is a measure of the length of the longest crack that was involved in a linkup event. For consistency, it is measured from the center of the extreme rivet to the crack tip, as illustrated in Figure 2-4. This definition insures proper evaluation of the size of the crack required to link up with a crack with the average maximum precursor length.

At the end of each simulation, data was collected on the following parameters: the number of cycles to the first initiation, the number of cycles to the first linkup, the number of cycles to the final linkup (ligament failure across the entire bay), the maximum precursor length for each linkup, the final crack size (to the nearest inch, as determined by the number of consecutive failed ligaments) of each linkup, the number of cycles from the time a linkup occurred until at least one of its ends had reinitiated (as shown in Figure 2-5), and the number of cycles from the time a linkup occurred until final linkup.

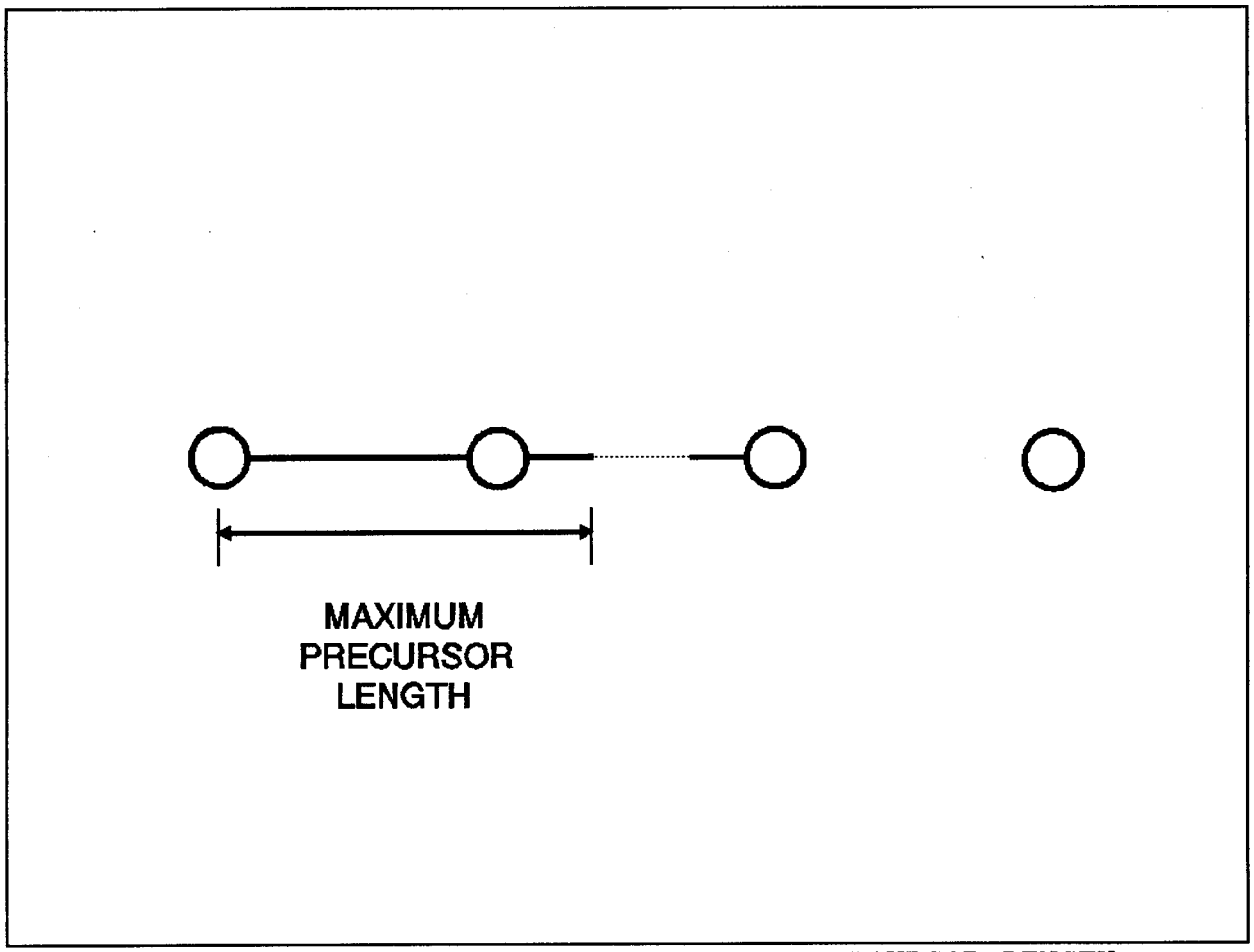

FIGURE 2-4. DEFINITION OF MAXIMUM PRECURSOR LENGTH

2.2 RESULTS OF THE SIMULATION

The program ran 10,000 simulations. The results for the entire bay included average number of cycles to first initiation, average number of cycles to first linkup, and average number of cycles to final linkup. These are given in Table 2-3. For each linkup containing an integral number of ligaments, the data included the average maximum precursor length, the average number of cycles until reinitiation, and the average number of cycles to final linkup. Reinitiation is the event when at least one end of the crack has initiated a sharp crack tip past the rivet. These results are given in Table 2-4.

2.3 DISCUSSION OF THE SIMULATION

The crack initiation and growth models combined to create this simulation are extrapolated from data on test specimens that are, at best, similar to the Boeing 737 lap joint. Nonetheless, the errors are unlikely to be entirely cumulative and the results

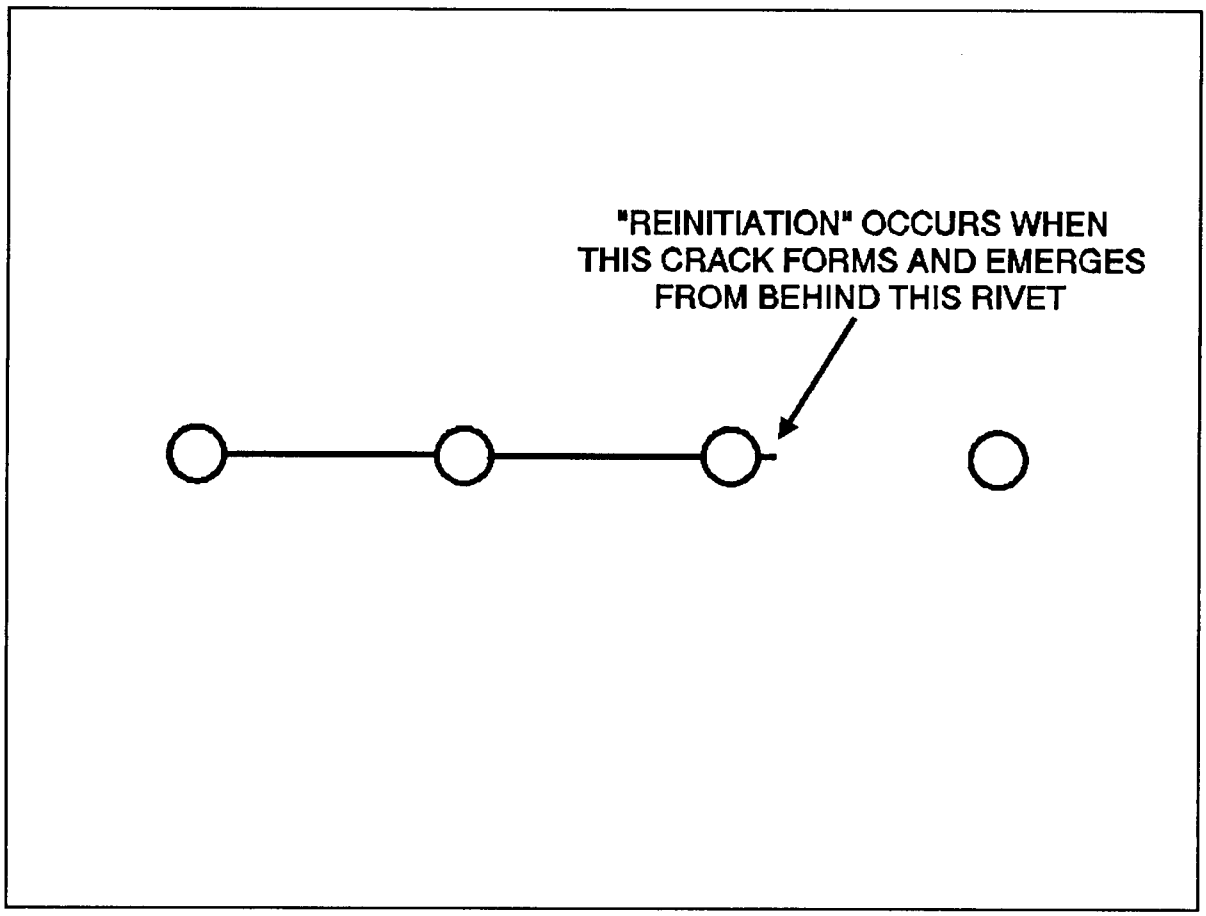

FIGURE 2-5. DEFINITION OF CRACK REINITIATION

TABLE 2-3. AVERAGE RESULTS FOR THE ENTIRE BAY

Average Cycles to First Initiation	47,922
Average Cycles to First Linkup	78,271
Average Cycles to Final Linkup	79,380
Average Maximum Precursor Length for Final Linkup	4.188

should give a better understanding of the crack initiation and growth history than a simple single crack model would.

The results of the simulation imply that most of the life of a bay of rivets (even after adhesive bond failure) is spent with no initiated cracks. After cracks initiate, many cycles elapse before they begin to link up. However, once a linkup occurs, final linkup across the entire bay occurs quickly. Thus, if the complete

TABLE 2-4. AVERAGE RESULTS FOR LINKUPS

Number of Ligaments	Number of Events	Average Maximum Precursor Length [inches]	Average Number of Cycles to Reinitiation	Average Number of Cycles to Final Linkup
1	4,294	0.56	3	1,256
2	7,676	1.02	16	1,035
3	4,180	2.29	1	447
4	4,225	2.91	0	305
5	2,506	3.58	0	193
6	2,216	4.00	1	34
7	54	5.08	0	118
8	10	4.24	0	125
9	7	5.57	0	125

debonding assumption is reasonable, intermediate length cracks (longer than one ligament length but less than the width of the bay) spend little time at that size. That any cracks of this size are found suggests a high probability of detection.

Although it might seem counterintuitive that so much of the damage happens in such a small fraction of the structure's fatigue life, these results correlate favorably with a fatigue test run by Foster-Miller, Inc. on a full-scale fuselage panel [11]. The panel did not have an adhesive layer between the skins in the lap joint region. Figure 2-6 shows the approximate size of cracks detected at various numbers of cycles before failure. In less than 5300 cycles, the damage state in the panel progressed from one relatively small crack to a multiple bay failure.

An important caveat regarding both the simulation and the test is that they assume complete adhesive failure. In actual service, the degree of adhesive failure depends on the aircraft's loading and on the manufacturing process used. Perfect bonding would relieve nearly all of the load transfer from the rivets. The stress concentration would remain at the edges of the holes, although the nominal stress level would be about half the far field stress level. Crack initiation would be delayed and subsequent growth would be slower. Progressive disbond of the adhesive might allow larger crack sizes to be more stable.

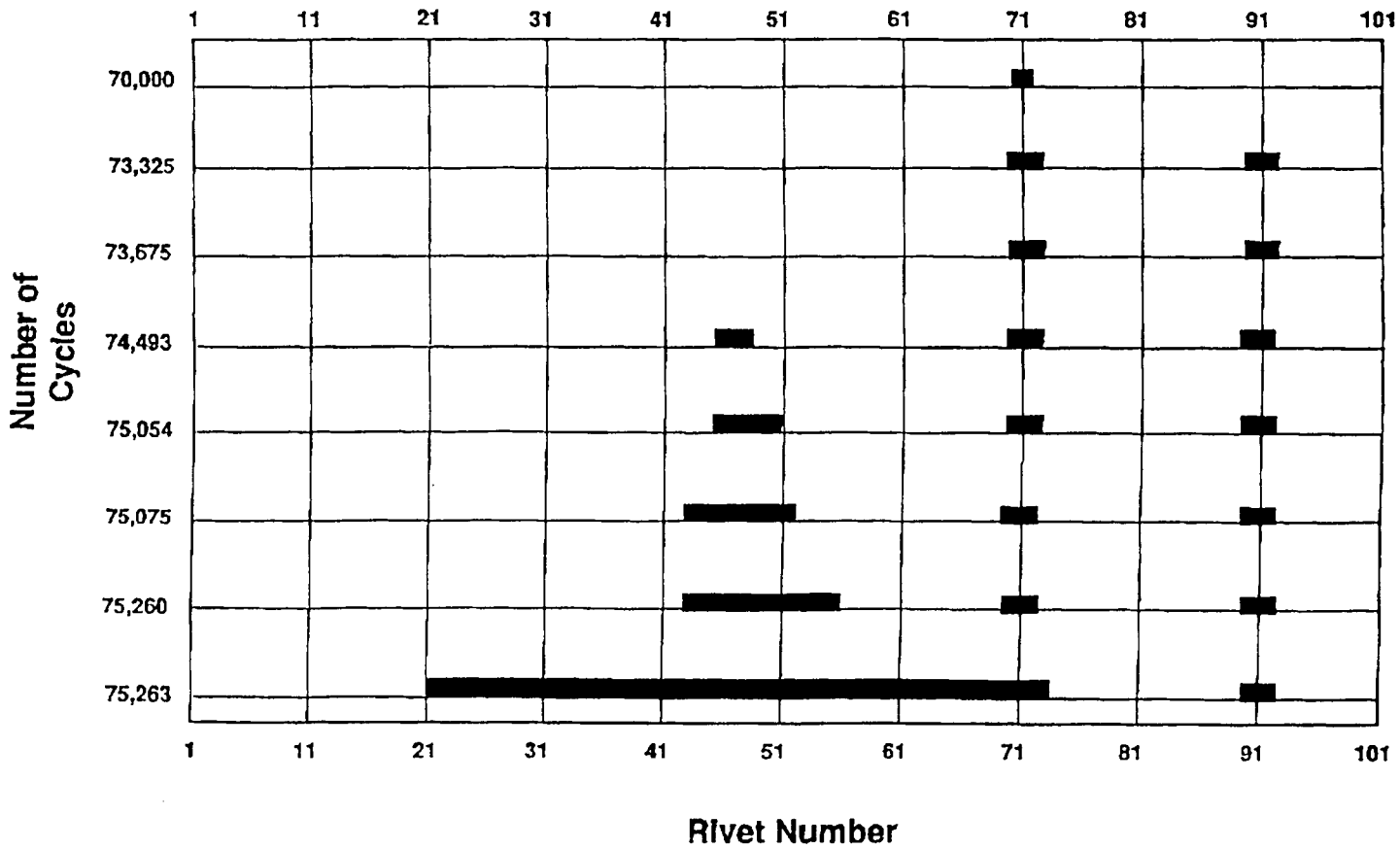

FIGURE 2-6. CRACK SIZE DISTRIBUTION IN A FATIGUE TEST OF A FULL-SCALE FUSELAGE PANEL

3. NOMINAL CRACK GROWTH HISTORIES

3.1 DETERMINATION OF NOMINAL CRACK GROWTH HISTORIES

The "nominal" history of a crack was calculated by growing it "backwards in time" using the same crack growth model that had been used in the simulation. The nominal crack growth behavior was computed for each crack size that traversed an integral number of ligaments (i.e., one through nine inches). When a crack tip grew back under a rivet head and underwent the average reinitiation period, it was assumed to "unlink." It was then replaced by a crack equivalent to its average maximum precursor length and another smaller crack. The length of the smaller crack was computed to be that which would link up with the average maximum precursor crack.

Since there were stochastic components of the original crack growth model (e.g., the rivet interference parameter, δ_o), each crack was analyzed 100 times. Its average size as a function of time was then computed. The nominal crack growth behaviors of cracks one through nine ligaments long are tabulated in Appendix A. The example of a four-ligament crack is shown in Figure 3-1.

When the results in Appendix A are applied, it should be assumed that detection events for cracks of integral ligament length occur in the middle of the period of reinitiation. However, since the average number of cycles to reinitiation for all crack sizes was quite small, this is effectively equivalent to assuming that each crack had just linked up when it was detected.

3.2 DISCUSSION OF NOMINAL CRACK GROWTH HISTORIES

The nominal crack growth histories in Appendix A give a representation of the crack growth behavior of large cracks. They include the contributions of random crack initiation, realistic stress distributions, linkup phenomena, and rivet interference. Although this initial study of these contributions reveals important trends, experimental data for the specific configuration modeled would enhance the accuracy of the simulation.

This methodology condenses the results of a simulation to assess average behavior. Unfortunately, the variations that are important in the characterization of nominal behavior may also have significant implications when calculating POD curves. A more accurate method for generating nondetection events in a POD analysis would be a "backwards simulation" of each detected crack. That is, instead of assuming an average (nominal) value for the maximum precursor length when a crack unlinks, a value would be selected via a random number generator using data produced by the simulation. That approach may be too computationally intensive to

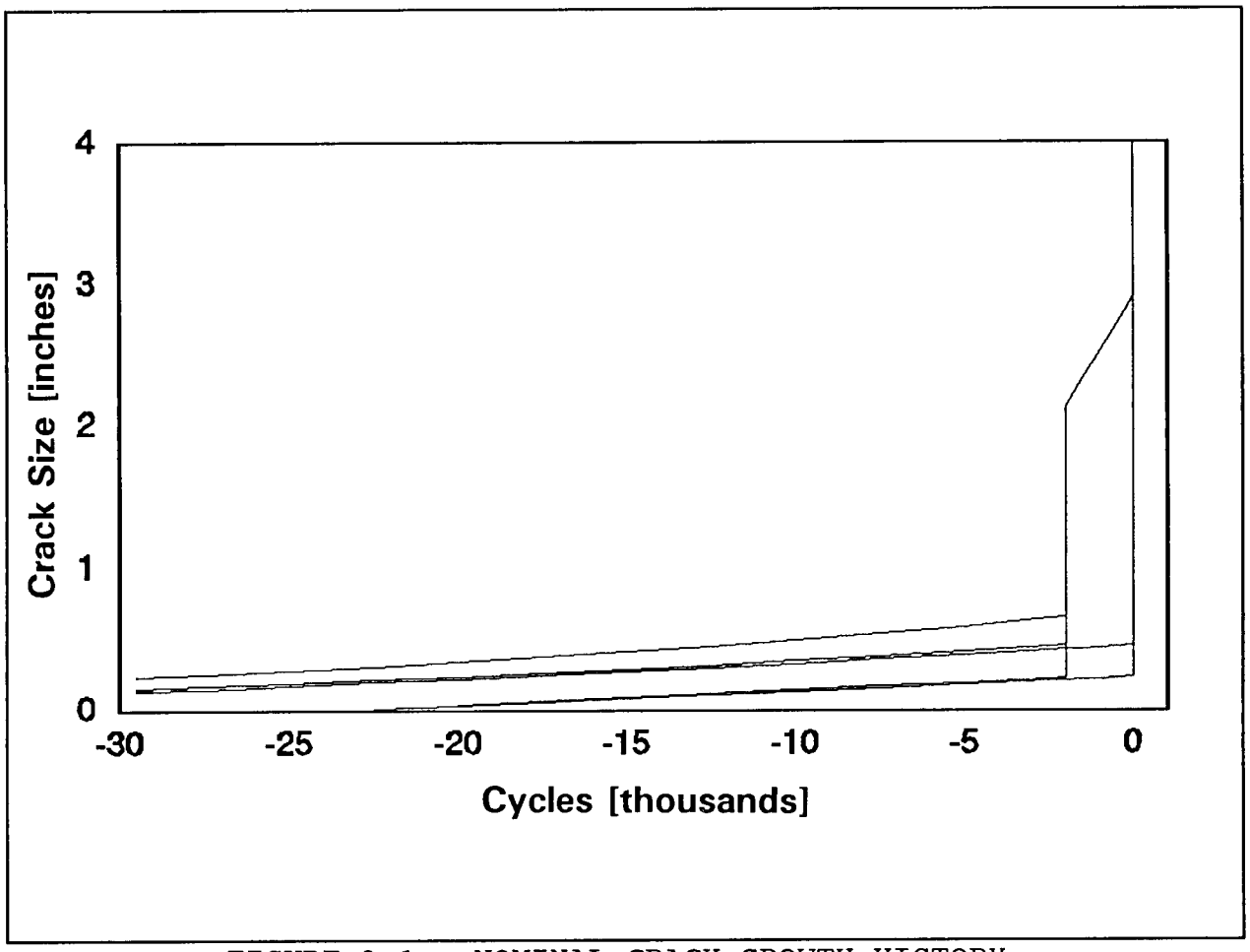

FIGURE 3-1. NOMINAL CRACK GROWTH HISTORY OF A FOUR-LIGAMENT CRACK

be practical. Nonetheless, it is likely, for example, that a significant fraction of four-inch cracks linked up from precursor cracks more than three inches long. The nominal value for maximum precursor length is 2.91 inches.

4. ANALYSIS OF DATA FROM SERVICE DIFFICULTY REPORTS

4.1 THE SERVICE DIFFICULTY REPORT DATABASE

The Service Difficulty Report (SDR) database is maintained by the Federal Aviation Administration (FAA) in Oklahoma City, OK. It contains reports on incidents of problems or damage to all aircraft in the transport aircraft fleet. These reports are not limited to structural damage entries used in this work.

The relevant data for the period March 1985 through March 1992 was obtained by Dr. Chris Smith of the FAA Technical Center. He restricted the data to include only skin cracks found on Boeing 737's during "C" level inspections. Boeing 737's were chosen because the lap joint was the structure most closely modeled by the simulation and nominal crack growth histories. "C-checks" were specified because they represented a common and well-known level of inspection. "D-checks" and directed inspections (e.g., those required by manufacturers' Service Bulletins and FAA Airworthiness Directives) were specifically omitted because they were far less frequent (and would therefore have fewer valid nondetection events) and the inspectors were inherently more focused on particular defects.

The frequency of a Boeing 737 C-check is approximately once every 2000 flight hours, or about once each year. The assumed inspection interval in this analysis was one year. In terms of flight cycles, it was assumed to be 2500 cycles.

The program that extracted the data listed 632 separate crack detection events. In cross-checking the data with the data file that contained all the Boeing 737 skin crack data, it was found that many events were erroneously repeated. These events were removed. Detected cracks less than 0.2" long were also removed. The comments section of one event stated that the crack was in skin near a wing engine pylon, so the event was removed. Finally, when multiple cracks were listed under a single entry, the extraction program counted each crack as a separate detection event with the longest listed length. Usually, this was acceptable within the limits of the accuracy of the database. In two cases involving major cracks, the number of cracks and range of sizes warranted adjusting the crack sizes. A group of four cracks one to four inches long was changed from four four-inch cracks to a one-inch crack, a two-inch crack, a three-inch crack, and a four-inch crack. A group of six cracks 0.5" to 1.5" long was changed from six 1.5" cracks to a 0.5" crack, a 0.75" crack, a 1.0" crack, a 1.25" crack, and two 1.5" cracks. This process yielded 329 crack detection events.

An important attribute of the SDR database is the limited precision of the crack lengths. In almost all cases, the crack lengths were listed as simple rational fractions of an inch. It was not clear whether the lengths were measured from the edge or center of the rivet. The convention used in this analysis was that cracks less than an inch long (one rivet spacing) were assumed to have been measured from the edge of the rivet (the visible portion of the crack) and that cracks over an inch long were assumed to have been measured from the center of a rivet. Fatigue crack growth can be so slow that a small percentage difference in length can represent a significant difference in life. Nonetheless, it must be assumed that results from the actual distribution can be adequately represented by the recorded data.

4.2 APPLICATION OF THE "KEEP REGION"

Two crack growth methodologies were used to analyze the crack detection data. The first was the Walker model described by Equation 2-4. Each crack was modeled as a simple center crack with two active crack tips in an infinitely wide flat sheet. The second was the nominal crack growth history methodology described in Section 3. In both cases, the detection events and the associated nondetection events of uncensored data would inappropriately represent the actual ratio of detections to nondetections for any arbitrary range of crack lengths. There would be valid nondetection events that are associated with cracks that had not been found by the closing of the database. There would be valid detections that would not be included because they occurred before the opening of the database. For this reason, only detection and nondetection events that occurred within the "keep region" defined in Figure 1-2 were considered in these analyses.

It is straightforward to eliminate (i.e., refrain from generating) the nondetection events that occur before the database opens. For a detection event to be within the keep region, it must be of such a size that it would have reached an obviously detectable size before the close of the database. The obviously detectable size was assumed to be ten inches (the width of one bay). The minimum crack sizes as a function of number of inspection periods (years) before the closing of the database are given for the two crack growth methodologies in Table 4-1.

If each of the 329 detection events were allowed to generate all possible nondetection events associated with cracks greater than 0.2" long, there would be 3356 nondetection events when the nominal crack growth history method was used. With a well-defined keep region, there were 86 detection events and 167 nondetection events. When the Walker crack growth equation was used, there were 43 detection events and 100 nondetection events.

TABLE 4-1. MINIMUM CRACK SIZES NECESSARY TO BE IN THE "KEEP REGION"

Number of Inspection Periods until Closure of Database	Walker Crack Growth Equation [inches]	Nominal Crack Growth History [inches]
0	10.00	10.00
1	3.65	1.54
2	2.23	0.63
3	1.61	0.58
4	1.26	0.53
5	1.03	0.49
6	0.87	0.44

4.3 MAXIMUM LIKELIHOOD ESTIMATE OF PROBABILITY OF DETECTION

The detection and nondetection data from both models were analyzed using the SAS software program. SAS gives several functional forms that can be used to describe the probability of crack detection. For completeness, five different fits will be described. Some fits (e.g., log normal) are merely applications of a standard fit to the logarithm of the crack size. This yields desirable qualities at the extremes because the POD will go identically to zero at a crack size of zero and will more slowly approach unity as the crack size becomes large. Nonetheless, the extrapolation of any of these functions out of the range of actual data should be discouraged.

The functional forms are expressed in terms of a shape parameter, α, and a location parameter, β. The logistic fit expresses POD as:

$$POD = \frac{1}{1 + e^{(\alpha a + \beta)}} \tag{4-1}$$

where a is the crack size. The log logistic fit, therefore, expresses POD as:

$$POD = \frac{1}{1 + e^{(\alpha \ln(a) + \beta)}} \tag{4-2}$$

The log Gompertz (Weibull) fit expresses POD as:

$$POD = e^{\left(-e^{(\alpha \ln(a) + \beta)}\right)} \tag{4-3}$$

The normal distribution requires the use of the function $\Phi(x)$, which describes the probability that a random number will fall between $-\infty$ and x. For example, if the mean of a normal distribution is zero, $\Phi(0) = 0.5$ indicates that half of all numbers randomly chosen from the distribution will fall below the mean. The shape and location parameters are traditionally expressed as the standard deviation, σ, and the mean, μ. The general expression for $\Phi(x)$ is:

$$\Phi(x) = \int_{-\infty}^{x} \frac{1}{\sqrt{2\pi}\,\sigma} e^{-\left(\frac{(x-\mu)^2}{2\sigma^2}\right)} dx \tag{4-4}$$

The expression for POD using a normal distribution is then:

$$POD = \Phi\left(\frac{a-\mu}{\sigma}\right) \tag{4-5}$$

For a log normal distribution, POD becomes:

$$POD = \Phi\left(\frac{\ln(a) - \mu}{\sigma}\right) \tag{4-6}$$

The maximum likelihood parameters calculated by SAS are given for both crack growth methodologies in Table 4-2. Figure 4-1 is a plot of the POD functions for the nominal crack growth history methodology. Figure 4-2 is a plot of the POD functions for the Walker crack growth methodology. For clarity, only the logistic, log normal, and Weibull distributions are shown. Figures 4-1 and 4-2 also contain some "histogram" data points that were derived by splitting the detection and nondetection events into ranges of crack sizes and estimating the POD for that range by dividing the number of detections into the total number of events. Events exactly at the boundary of the range were counted as half events. Table 4-3 contains the histogram data for the nominal crack growth history methodology. Table 4-4 contains the histogram data for the Walker crack growth methodology.

TABLE 4-2. MAXIMUM LIKELIHOOD SHAPE AND LOCATION PARAMETERS FOR PROBABILITY OF DETECTION FUNCTIONS

Functional Form of POD	Walker Crack Growth Equation		Nominal Crack Growth History	
	Shape Parameter (α,σ)	Location Parameter (β,μ)	Shape Parameter (α,σ)	Location Parameter (β,μ)
Normal	1.55	2.90	0.30	0.98
Log Normal	0.63	0.97	0.34	-0.09
Logistic	-1.08	3.10	-5.97	5.72
Log Logistic	-2.66	2.58	-5.33	-0.53
Log Gompertz (Weibull)	-1.65	1.16	-3.10	-0.81

Note: These parameters assume *a* is measured in inches.

4.4 DISCUSSION OF THE MAXIMUM LIKELIHOOD ESTIMATES

For each of the crack growth methodologies, there is little variation among the five functional forms of the POD curves. They each give a good fit to the histogram data. Figure 4-3 shows the difference between the results for the two methodologies. For clarity, only the logistic fit is shown.

TABLE 4-3. HISTOGRAM ESTIMATES OF POD FOR NOMINAL CRACK GROWTH HISTORY METHODOLOGY

Range of Crack Sizes [inches]	Number of Events	Histogram POD
0.5-0.75	125.5	0.06
0.75-1.25	34.5	0.80
1.25-1.75	14	0.79
1.75-2.25	10.5	1.00
>2.25	26.5	1.00

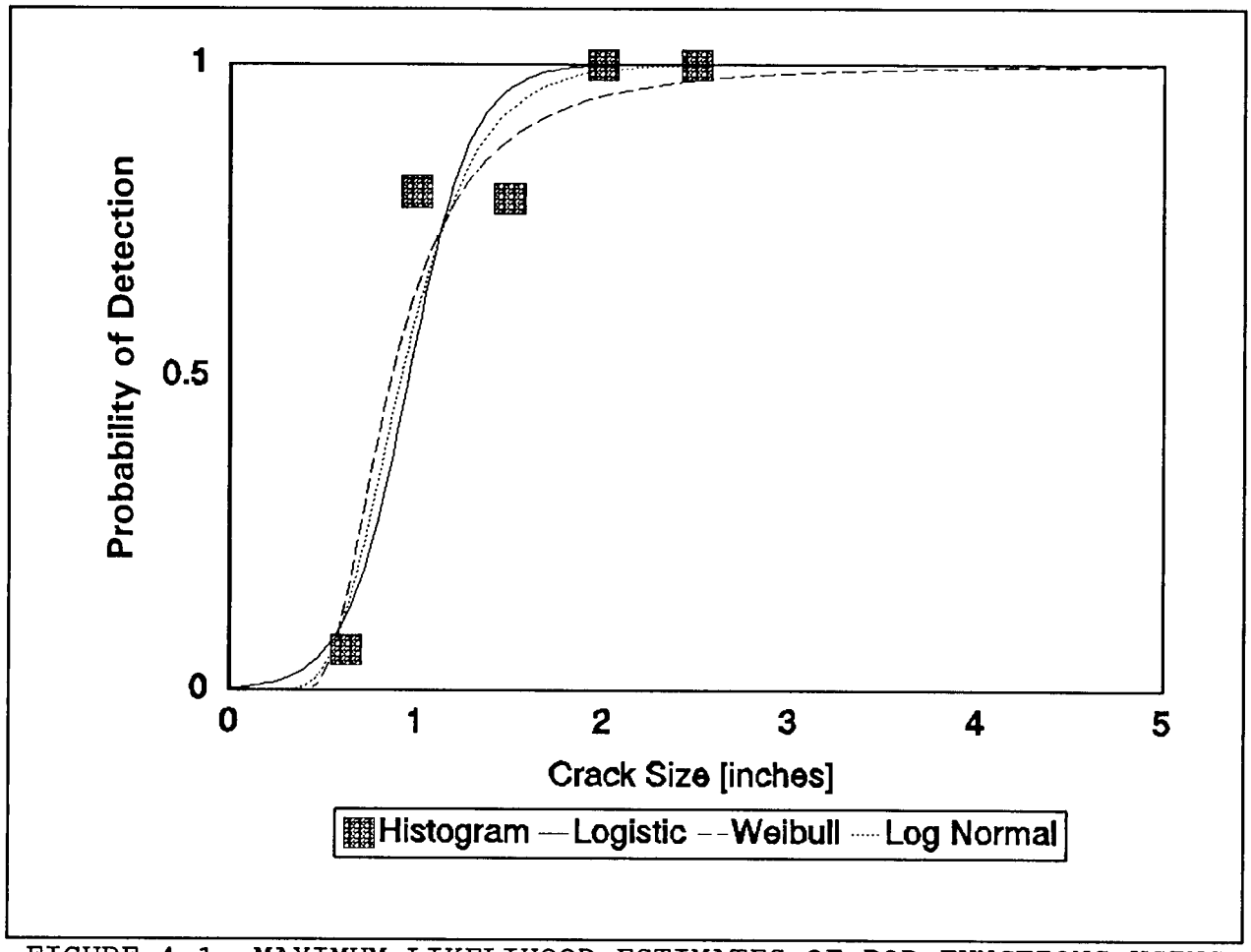

FIGURE 4-1. MAXIMUM LIKELIHOOD ESTIMATES OF POD FUNCTIONS USING THE NOMINAL CRACK GROWTH HISTORY METHODOLOGY

The Walker crack growth methodology gives a higher POD for small crack sizes and a lower POD for large crack sizes. The POD is generally lower over most of the range of crack sizes. This behavior can be explained with some fundamental observations of the two crack growth methodologies. The nominal crack growth history methodology assumes slow initial growth with linkup eventually causing rapid growth. Over the range of crack sizes in the censored data, the effective growth rate was much faster than with the Walker methodology. Hence, the methodology generated few nondetection events at large crack sizes. This causes the estimated POD to increase in this range. There is compensation for this effect because the slower crack growth with the Walker model implies that there are more opportunities for detection (i.e., more inspections) between the time it is first detectable and the time that it extends across an entire bay. Thus, the effect on a damage tolerance analysis is uncertain and should be investigated.

The disparity between the POD curves produced by the two methodologies might be employed to draw conclusions about crack

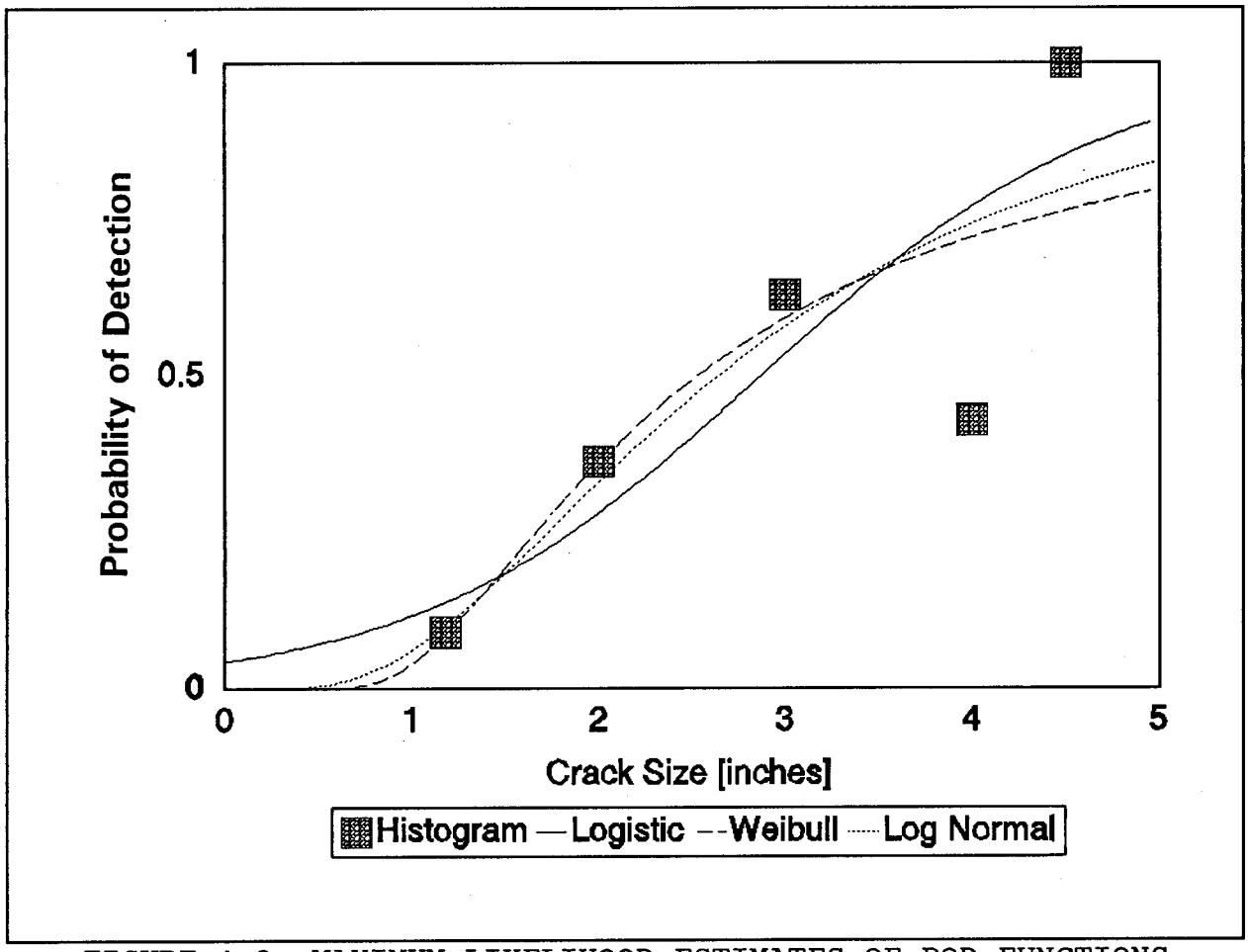

FIGURE 4-2. MAXIMUM LIKELIHOOD ESTIMATES OF POD FUNCTIONS USING THE WALKER CRACK GROWTH METHODOLOGY

growth in the fleet. If the in-service POD at C-checks could be reliably estimated by an independent method, it would probably fall closer to one of these curves than the other. It could then be inferred which methodology better represents crack growth in the fleet. Since the nominal crack growth history methodolgy predicts widespread fatigue damage and the Walker equation methodology assumes growth of a single crack, the significance of widespread fatigue damage in the fleet might be deduced.

An implication of the nominal crack growth history methodology is that there are numerous nondetection events for small crack sizes (on the order of 0.25"). Although many detection events were listed in the database, both the detection and nondetection events were below the minimum crack size needed to be included in the keep region. This allowed the estimated POD to approach zero for 0.25" cracks. This value could be appropriate, however, if a database of longer duration generated enough nondetection events in that range.

TABLE 4-4. HISTOGRAM ESTIMATES OF POD FOR WALKER CRACK GROWTH METHODOLOGY

Range of Crack Sizes [inches]	Number of Events	Histogram POD
0.85-1.5	67	0.09
1.5-2.5	47	0.36
2.5-3.5	13.5	0.63
3.5-4.5	7	0.43
>4.5	8.5	1.00

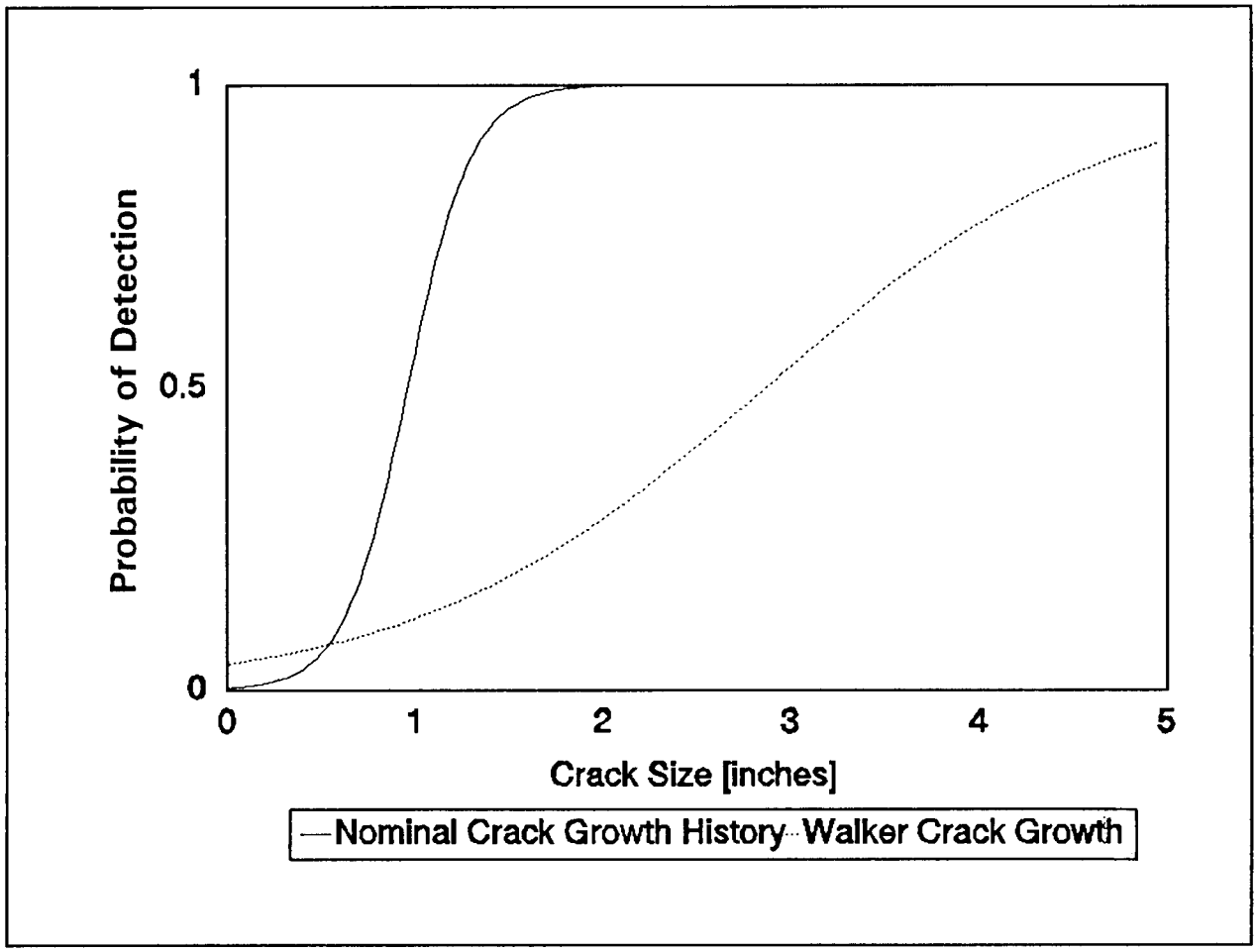

FIGURE 4-3. COMPARISON OF THE PROBABILITY OF DETECTION CURVES FROM THE TWO METHODOLOGIES (LOGISTIC FIT ONLY)

The Walker methodology is simpler to apply and results in probabilities of detection for extreme crack sizes that seem more intuitively correct. That is, the POD is greater than zero for small cracks that are often found and is less than unity for large cracks. Nonetheless, crack growth in a lap joint is more

complicated than a simple crack growth equation can describe. Thus, the description of the events at extreme crack sizes may be dubious. If the nominal crack growth history methodology generates fewer nondetection events than it should, it is probably because the present version does not fully account for the stability in large crack sizes caused by partial debonding of bays. Or, it could also occur because this version cannot account for the potentially significant behavior of the non-nominal slow-growing cracks seen in the simulation. There is also a need to extend the period of the database to perhaps 15 years in order to generate enough nondetection events at small crack sizes.

It is most likely, therefore, that neither methodology in its present form gives a good representation of the POD for extreme crack sizes. Nonetheless, the nominal crack growth history methodology should give reasonable results for a midrange of crack sizes. This might be verified with simulations that include inspections. Crack growth in a bay could be simulated with the two methodologies and monitored with inspection methods with the appropriate POD properties. A good model should deliver a distribution of detection events similar to that of the SDR data.

The Walker crack growth methodology should give a lower bound to POD. It is unlikely that cracks would grow more slowly than that unless the bonding is completely intact. In those cases, few cracks are likely to arise and those that do could well initiate debonding. Unfortunately, the POD generated by the Walker approach might be far too conservative to be practical. An alternative might be to use the lower of the two POD curves in the regions of extreme crack sizes. A third approach is suggested by the two histogram points in Figure 4-1 at approximately 0.8. If the two points at 1.0 result from the present model's inability to model the effects of partial debonding, then perhaps in-service POD is limited to a maximum of 80%. Then a reasonable estimate of a true POD curve might be the POD curve from the nominal crack growth history methodology multiplied by 0.8.

5. CONCLUSIONS AND RECOMMENDATIONS

The work described in this report supports the following conclusions:

1. The nominal crack growth histories produced in this work are better representations of how cracks initiate, grow, and link up than simple single-crack analyses using a conventional crack growth model.

2. The multiple-crack linkup model predicts that cracks remain short for most of their lives. Once the cracks start linking up, substantial growth is almost immediate.

3. Damage tolerance analyses must carefully consider this effect. A single-crack analysis using a simple crack growth equation gives a conservative probability of detection function. However, because it predicts a longer time at large crack sizes, it may not give a conservative estimate of the cumulative probability of crack detection or the time necessary to grow from a minimally detectable crack to a critical crack.

4. The probability of detection curves produced with the nominal crack growth history methodology are most applicable in the midrange of probabilities. Further extensions of the details of the model and the duration of the database may be needed to resolve the probability of detection for extreme crack sizes.

Although the methodology described in this report represents an advance over simple crack growth models, there are further improvements that can be made to each component of the simulation and analyses that can be performed to assess its accuracy. Therefore, the following recommendations are made:

1. Most components of the simulation would benefit from additional data that relates to the specific structural component being analyzed.

2. The addition of the effect of partially versus fully debonded bays of a lap joint should be investigated.

3. The possibility of using an efficient stochastic simulation for generating nondetection events from detection data should also be considered.

4. The present approach should be assessed by using the probability of crack detection curve generated from the maintenance data in a simulation of growth and inspection. If the distribution of detected crack sizes is similar between the simulation and the maintenance data, then the approach will be self-consistent. The

results could be compared with similar simulations using the Walker methodology and the POD curve from the nominal crack growth history methodology multiplied by 0.8.

5. Independent estimates of the in-service probability of crack detection at C-checks should be used to infer qualitatively the frequency of widespread fatigue damage in the population of cracks in the fleet.

REFERENCES

1. Federal Aviation Administration Advisory Circular 25.571-1A. March 5, 1986.

2. Brewer, J. C., and P. Mengert. *Preliminary Output of the Aircraft System Reliability Analysis*. Project Memorandum DOT-VNTSC-FA3H2-PM-93-13. September 1992.

3. Canha, J. V., Jr. *Aircraft Section Model for Strain Field Characterization*, Volpe Center Technical Interchange Document for FAA Technical Center. April 1993.

4. Broek, D. "Outline of Risk Analysis to Establish Requirements for Inspection Interval." *FractuREsearch Technical Note 9104*. July 1991.

5. Hartman, A. *Fatigue Tests on 3-Row Lap Joints in Clad 2024-T3 Manufactured by Riveting and Adhesive Bonding*. National Aerospace Laboratory (NLR), Amsterdam, The Netherlands, Report TN M-2170, 1967.

6. Schijve, J. "The Endurance under Program Fatigue Testing," *Full Scale Fatigue Testing of Aircraft Structures*. Pergamon, 1961, pp.41-59.

7. Brewer, J. C. *Preliminary Correlation of Crack Growth Data Using Rivet Interference Effects*. Volpe National Transportation Systems Center Letter Report LTR-FA3H2-9301, April 1993.

8. *Damage Tolerance Assessment Handbook, Volume 1*, Volpe National Transportation Systems Center, April 1993, pp. 3-27.

9. Partl, O., and J. Schijve. "Multiple-site Damage in 2024-T3 Alloy Sheet." *International Journal of Fatigue*, Vol. 15, No. 4, pp. 293-299.

10. Jeong, D. *Correlation of Residual Strength Tests with Analysis*. Volpe National Transportation Systems Center Report, in preparation.

11. Thomson, D., G. Samavedam, D. Hoadley, and D. Jeong. *Aircraft Fuselage Lap Joint Fatigue and Terminating Action Repair*. Federal Aviation Administration Technical Center Report. August 1993.

APPENDIX A

NOMINAL CRACK SIZES (DOWN TO 0.1") THAT PRECEDE OBSERVED CRACKS

NOTE: CRACK LENGTHS LISTED AS MORE THAN ONE INCH ARE MEASURED FROM THE CENTER OF THE RIVET AT THE UNCRACKED END. CRACK LENGTHS LISTED UNDER ONE INCH ARE MEASURED FROM THE EDGE OF THE RIVET.

TABLE A-1. NOMINAL HISTORY OF A ONE-INCH CRACK

CYCLES BEFORE DETECTION	CRACK SIZES [in.]	
0	1.00	
1	0.46	0.23
2500	0.42	0.20
5000	0.39	0.18
7500	0.36	0.15
10000	0.33	0.12
12500	0.30	0.10
15000	0.27	
17500	0.25	
20000	0.22	
22500	0.20	
25000	0.18	
27500	0.16	
30000	0.13	
32500	0.11	
35000	0.09	

TABLE A-2. NOMINAL HISTORY OF A TWO-INCH CRACK

CYCLES BEFORE DETECTION	CRACK SIZES [in.]		
0	2.00		
8	1.02		0.66
9	0.46	0.23	0.66
2500	0.42	0.20	0.60
5000	0.39	0.18	0.55
7500	0.36	0.15	0.50
10000	0.33	0.12	0.46
12500	0.30	0.10	0.42
15000	0.27		0.38
17500	0.25		0.35
20000	0.22		0.32
22500	0.20		0.29
25000	0.18		0.26
27500	0.16		0.23
30000	0.13		0.21
32500	0.11		0.18
35000	0.09		0.16
37500			0.13
40000			0.11
42500			0.08

TABLE A-3. NOMINAL HISTORY OF A THREE-INCH CRACK

CYCLES BEFORE DETECTION	CRACK SIZES [in.]			
0	3.00			
1	2.29			0.50
456	0.66	0.46	0.23	0.49
2500	0.62	0.43	0.21	0.46
5000	0.57	0.39	0.18	0.42
7500	0.52	0.36	0.15	0.38
10000	0.48	0.33	0.13	0.35
12500	0.44	0.30	0.10	0.32
15000	0.41	0.28		0.29
17500	0.38	0.25		0.26
20000	0.35	0.23		0.23
22500	0.32	0.20		0.21
25000	0.29	0.18		0.18
27500	0.27	0.16		0.16
30000	0.24	0.14		0.13
32500	0.22	0.12		0.11
35000	0.20	0.10		0.08
37500	0.18			
40000	0.16			
42500	0.13			
45000	0.11			
47500	0.09			

TABLE A-4. NOMINAL HISTORY OF A FOUR-INCH CRACK

CYCLES BEFORE DETECTION	CRACK SIZES [in.]				
0	4.00				
1	2.91			1.00	
2	2.91			0.46	0.23
2039	1.00		0.66	0.43	0.21
2040	0.46	0.23	0.66	0.43	0.21
2500	0.45	0.22	0.65	0.42	0.21
5000	0.42	0.20	0.59	0.39	0.18
7500	0.38	0.17	0.54	0.36	0.16
10000	0.35	0.14	0.49	0.33	0.13
12500	0.32	0.12	0.45	0.30	0.11
15000	0.29	0.10	0.41	0.27	0.08
17500	0.27		0.38	0.25	
20000	0.24		0.34	0.22	
22500	0.22		0.31	0.20	
25000	0.19		0.28	0.17	
27500	0.17		0.25	0.15	
30000	0.15		0.23	0.13	
32500	0.13		0.20	0.11	
35000	0.11		0.18	0.08	
37500	0.09		0.15		
40000			0.13		
42500			0.10		

TABLE A-5. NOMINAL HISTORY OF A FIVE-INCH CRACK

CYCLES BEFORE DETECTION	CRACK SIZES [in.]					
0	5.00					
1	3.58				1.16	
322	3.34				0.46	0.23
603	0.42	2.29			0.45	0.23
1011	0.41	0.66	0.46	0.23	0.45	0.23
2500	0.39	0.63	0.44	0.21	0.43	0.21
5000	0.37	0.58	0.40	0.19	0.39	0.19
7500	0.34	0.53	0.37	0.16	0.35	0.16
10000	0.31	0.49	0.34	0.13	0.32	0.14
12500	0.29	0.45	0.31	0.11	0.29	0.12
15000	0.27	0.42	0.28	0.08	0.26	0.10
17500	0.24	0.38	0.26		0.24	
20000	0.22	0.35	0.23		0.21	
22500	0.20	0.32	0.21		0.19	
25000	0.18	0.30	0.19		0.16	
27500	0.16	0.27	0.17		0.14	
30000	0.14	0.25	0.14		0.11	
32500	0.13	0.23	0.12		0.09	
35000	0.11	0.20	0.10			
37500	0.09	0.18				
40000		0.16				
42500		0.14				
45000		0.12				
47500		0.10				

TABLE A-6. NOMINAL HISTORY OF A SIX-INCH CRACK

CYCLES BEFORE DETECTION	CRACK SIZES [in.]						
0	6.00						
1	4.00					1.61	
2	2.91			1.00		1.61	
3	2.91			0.46	0.23	1.61	
1958	1.02		0.66	0.43	0.21	1.39	
1959	0.46	0.23	0.66	0.43	0.21	1.39	
2500	0.45	0.22	0.64	0.43	0.21	1.32	
4095	0.43	0.20	0.61	0.41	0.20	0.46	0.24
5000	0.42	0.20	0.59	0.40	0.19	0.45	0.23
7500	0.38	0.17	0.54	0.37	0.17	0.41	0.21
10000	0.35	0.14	0.49	0.34	0.15	0.38	0.19
12500	0.32	0.12	0.45	0.31	0.13	0.34	0.17
15000	0.29	0.09	0.41	0.29	0.11	0.32	0.15
17500	0.27		0.38	0.27	0.09	0.29	0.13
20000	0.24		0.34	0.25		0.26	0.11
22500	0.22		0.31	0.22		0.24	0.09
25000	0.20		0.28	0.20		0.21	
27500	0.17		0.26	0.18		0.19	
30000	0.15		0.23	0.16		0.17	
32500	0.13		0.20	0.15		0.15	
35000	0.11		0.18	0.13		0.12	
37500	0.09		0.15	0.11		0.10	
40000			0.13	0.09			
42500			0.10				

TABLE A-7. NOMINAL HISTORY OF A SEVEN-INCH CRACK

CYCLES BEFORE DETECTION	CRACK SIZES [in.]							
0	7.00							
1	5.08						1.58	
2	1.17		3.58				1.58	
430	0.46	0.24	3.24				1.53	
581	0.46	0.24	2.29			0.50	1.51	
999	0.45	0.23	0.66	1.02		0.49	1.46	
1000	0.45	0.23	0.66	0.46	0.23	0.49	1.46	
2500	0.43	0.22	0.62	0.44	0.21	0.46	1.29	
3795	0.42	0.21	0.60	0.42	0.20	0.45	0.46	0.24
5000	0.41	0.20	0.58	0.40	0.19	0.43	0.44	0.23
7500	0.38	0.18	0.53	0.37	0.16	0.39	0.41	0.21
10000	0.36	0.16	0.49	0.34	0.13	0.35	0.37	0.18
12500	0.33	0.14	0.45	0.31	0.11	0.32	0.34	0.16
15000	0.31	0.12	0.42	0.28	0.08	0.29	0.31	0.14
17500	0.29	0.10	0.38	0.26		0.26	0.29	0.12
20000	0.27		0.35	0.23		0.24	0.26	0.10
22500	0.25		0.33	0.21		0.21	0.23	
25000	0.23		0.30	0.19		0.18	0.21	
27500	0.21		0.27	0.16		0.16	0.19	
30000	0.19		0.25	0.14		0.13	0.16	
32500	0.17		0.23	0.12		0.11	0.14	
35000	0.16		0.20	0.10		0.09	0.12	
37500	0.14		0.18				0.10	
40000	0.12		0.16					
42500	0.11		0.14					
45000	0.09		0.12					
47500			0.10					

TABLE A-8. NOMINAL HISTORY OF AN EIGHT-INCH CRACK

CYCLES BEFORE DETECTION	CRACK SIZES [in.]								
0	8.00								
1	3.39				4.24				
113	3.31				2.91			1.00	
114	3.31				2.91			0.46	0.26
363	0.42	2.29			2.81			0.46	0.26
802	0.42	0.66	1.02		2.65			0.45	0.26
803	0.42	0.66	0.46	0.23	2.65			0.45	0.26
2226	0.40	0.63	0.44	0.22	1.02		0.66	0.43	0.25
2227	0.40	0.63	0.44	0.22	0.23	0.46	0.66	0.43	0.25
2500	0.40	0.63	0.44	0.21	0.23	0.46	0.65	0.43	0.25
5000	0.38	0.58	0.40	0.19	0.20	0.42	0.60	0.40	0.24
7500	0.35	0.54	0.37	0.17	0.18	0.38	0.56	0.37	0.23
10000	0.33	0.50	0.34	0.15	0.16	0.35	0.51	0.34	0.22
12500	0.30	0.46	0.31	0.13	0.14	0.31	0.47	0.32	0.21
15000	0.28	0.43	0.29	0.10	0.12	0.28	0.43	0.29	0.20
17500	0.26	0.40	0.26		0.10	0.26	0.40	0.27	0.20
20000	0.24	0.37	0.24			0.23	0.37	0.25	0.19
22500	0.22	0.34	0.21			0.20	0.34	0.22	0.18
25000	0.21	0.32	0.19			0.18	0.31	0.20	0.17
27500	0.19	0.29	0.17			0.15	0.28	0.18	0.16
30000	0.17	0.27	0.15			0.13	0.26	0.16	0.15
32500	0.15	0.25	0.13			0.11	0.23	0.14	0.14
35000	0.14	0.23	0.11			0.08	0.21	0.12	0.14
37500	0.12	0.21	0.09				0.18	0.10	0.13
40000	0.10	0.19					0.16		0.12
42500		0.17							

TABLE A-9. NOMINAL HISTORY OF A NINE-INCH CRACK

CYCLES BEFORE DETECTION	CRACK SIZES [in.]									
0	9.00									
1	5.57						3.00			
2	5.57						2.29			0.46
271	1.17		3.58				2.19			0.45
473	1.15		3.43				1.02		0.67	0.45
474	1.15		3.43				0.46	0.23	0.67	0.45
874	1.11		0.42	2.29			0.45	0.23	0.66	0.45
957	0.46	0.26	0.42	2.26			0.45	0.23	0.66	0.45
1286	0.46	0.26	0.41	0.66	1.02		0.45	0.22	0.65	0.45
1287	0.46	0.26	0.41	0.66	0.46	0.23	0.45	0.22	0.65	0.45
2500	0.45	0.25	0.40	0.63	0.44	0.21	0.43	0.21	0.63	0.44
5000	0.44	0.23	0.37	0.58	0.41	0.19	0.39	0.19	0.58	0.43
7500	0.43	0.21	0.34	0.54	0.37	0.16	0.36	0.17	0.54	0.42
10000	0.41	0.19	0.32	0.49	0.34	0.14	0.32	0.14	0.51	0.40
12500	0.40	0.17	0.29	0.46	0.31	0.11	0.29	0.12	0.47	0.39
15000	0.39	0.16	0.27	0.42	0.29	0.09	0.27	0.10	0.44	0.38
17500	0.38	0.14	0.25	0.39	0.26		0.24		0.41	0.37
20000	0.37	0.12	0.23	0.36	0.24		0.21		0.38	0.35
22500	0.36	0.11	0.20	0.33	0.21		0.19		0.35	0.34
25000	0.35	0.09	0.19	0.30	0.19		0.16		0.32	0.33
27500	0.34		0.17	0.28	0.17		0.14		0.30	0.32
30000	0.33		0.15	0.25	0.15		0.11		0.27	0.31
32500	0.32		0.13	0.23	0.13		0.09		0.25	0.30
35000	0.31		0.11	0.20	0.10				0.23	0.29
37500	0.30		0.09	0.18					0.21	0.28
40000	0.29			0.16					0.19	0.27

TABLE A-9. NOMINAL HISTORY OF A NINE-INCH CRACK (CONTINUED)

CYCLES BEFORE DETECTION	CRACK SIZES [in.]			
42500	0.28	0.14	0.17	0.26
45000	0.28	0.12	0.15	0.25
47500	0.27	0.10	0.13	0.24
50000	0.26		0.11	0.23
52500	0.25		0.09	0.22
55000	0.24			0.22
57500	0.23			0.21
60000	0.23			0.20
62500	0.22			0.19
65000	0.21			0.18
67500	0.20			0.17
70000	0.20			0.16
72500	0.19			0.16
75000	0.18			0.15
77500	0.17			0.14
80000	0.17			0.13
82500	0.16			0.12
85000	0.15			0.11
87500	0.15			0.11
90000	0.14			0.10
92500	0.13			
95000	0.12			
97500	0.12			
100000	0.11			
102500	0.10			

•U.S. GOVERNMENT PRINTING OFFICE:1994-600-273/00044